Electrical Resistivity and Physiochemical studies for groundwater contamination at waste dumping site: A case study for I-12 Sector, Islamabad, Pakistan

By

Asif Ullah

M. Phil, Hydrogeology (2021-2023)

DEPARTMENT OF EARTH SCIENCES

QUAID-I-AZAM UNIVERSITY, ISLAMABAD

CERTIFICATE OF APPROVAL

This dissertation by has carried out all research work related to thesis under my supervision at the Department of Earth Sciences and the work fulfils the requirement for award of M.Phil degree in hydrogeology.

RECOMMENDED BY

Dissertation Supervisor

Dr Faisal Rehman …….

Chairman of the Department

Dr. Aamir Ali …….

External Examiner ……

DEDICATION

This thesis is dedicated to my parents, who taught me that the best kind of knowledge to have is that which is learned for its own sake and even the largest task can be accomplished if it is done one step at a time. I also dedicate this dissertation to my project supervisor who always supported me throughout the tenure. I will always appreciate his concern

ACKNOWLEDGEMENT

Thanks to Allah Almighty who is a creator of all and there is no deity except Him. All the respects are for His Holy Prophet Muhammad (PBUH), who enabled us to recognize our creator.

On the behalf of my faith in Almighty Allah today I have reached at this point of my life where I have successfully completed my research work. I wish to pay my deepest gratitude to my supervisor, **Dr. Faisal Rehman**. He was there for me from the start. I am humbly thankful for all his concern towards my work and encouraging me to work in the field of particle physics. It is whole heartedly appreciated for all his encouragement even when the road got really tough for me. The present research work would, therefore, have never been completed without his proper guidance, regular supervision, and constant encouragement.

I also wish to pay my regards all the people, whose assistance was a milestone in the completion of this project, including my supportive mother, my teachers and all the family members. I have completed my research and this thesis only due to the support and encouragement of the above-mentioned people.

I offer my deepest sense of gratitude to my friends, especially Maryam Zakir, Zubair Ahmad, Shah Zaib Ahmad Shah, Faizan Sabir, Dr Faheem Ullah, Dr Hafeez ur Rahman and all my MPHIL classmates for their endless love, care and moral support during my study.

Asif Ullah

TABLE OF CONTENTS

TABLE OF CONTENTS

TABLE OF CONTENTS

List of Figures

List of Tables

ABSTRACT

An open dumping site is a major environmental issue that affects water, air, surface water, and ground water. Ground water is a valuable supply of water, yet it's contaminated by leachate, which includes numerous harmful chemical compounds. The purpose of this study was to look into the impacts of leachate on hydrology in the I-12 area of Islamabad. Four vertical electrical resistivity soundings (VES) were recorded using the Schlumberger electrode design, with two VES acquired upstream and two VES acquired downstream of the research region. In addition, five ERT profiles were obtained to explore the impacts of leachate on water.

Due to non-availability of borehole data, we compared the vertical sounding and electrical resistivity results to confirm the distribution of leachate in the subsurface. The VES were acquired over the ERT profiles. In ERT profiles the leachate are identifiable based on the encountered resistivity values. For the similar area the VES shows abnormal resistivity curves due to the existence of different contaminant in combination at one place. This simply explains the nature of leachate having variable resistive materials. In the inversion results the contaminated leachate distribution is variable and exists in patches. The maximum depth for the encountered contaminated leachate varies between 38-40 m. The resistivity range for the contaminated leachate ranges between 0-30 Ωm. This resistivity range was assigned based on the test profile, which was acquired in the open field near the dumpsite.

Forty-one points were selected for water sampling at different specific distances from the sites in the study area as well as surrounding area to check the extend of contaminated water. Then the samples were examined for seventeen parameters that included electrical conductivity (EC), total dissolved solids (TDS), pH, bicarbonate (HCO_3), calcium (Ca), magnesium (Mg), chloride (Cl), sulfate (SO_4), hardness, sodium (Na), potassium (K), fluoride (F), and arsenic (As), nitrate (NO_3), phosphate (PO_4), iron (Fe) and lead (Pb) to investigate the affected ground water quality.

The concentration of Arsenic with an average value 34.49 ranges from 7.89– 98.7 and that only 5% of the samples collected had arsenic concentrations within the WHO limit, while 95% of the samples exceeded the limit. The Gibbs plot indicate that the major controlling factor that change the groundwater chemistry is Rock dominance

and only three samples lie in atmospheric precipitation zone. The health risk assessment is done by Average daily dose (ADD), Hazard quotient (HQ) and Carcinogenic risk (CR). For irrigation purpose Sodium Adsorption Ratio (SAR), Sodium Percentage (Na%), Kelly's Ratio, Magnesium Adsorption Ratio (MAR) and Salinity Hazard analysis are done, and calculations shows that the groundwater is suitable for the use of irrigation. The water quality index analysis is performed by collecting groundwater samples in the study area. The water quality index analysis shows that 34% of the groundwater samples lie in the excellent class, 36% groundwater samples lie in good water quality class, 20% lie in poor class, 10% in very poor class and no sample lie in worse class. Nearly 95% of the groundwater samples analyzed have Hazard Quotient (HQ) values greater than 1, indicating a potential risk of adverse health effects from exposure to the analyzed substances. Only 5% of the samples have HQ values lower than 1, suggesting that the exposure to the analyzed substances in these samples is unlikely to result in significant health effects.

Chapter 1 Introduction

1.1. Fresh water

Aquatic system which is also called fresh water ecosystem has safe drinkable water. If we consider distribution of water by percentages of drinkable and non-drinkable we can say that land contains only 3% as drinkable and 97 % is non drinkable because of salinity. From that 3% drinkable or fresh water 70% exist in form of ice caps or glaciers and the remaining can be classified as

Lentic water (static): such as lakes, ponds and bogs

Lotic water (moving): streams, canals, rivers, channels

In Pakistan fresh water comes from rain as well as melting glaciers which act as fresh water reservoirs and flow in form of rivers down the country such as river Jhelum and Indus (largest)

1.2. Ground water

It is present in subsurface in cracks and pore spaces of between the particles or grains of rocks present in subsurface, rate of this groundwater flow is influenced by size of pore spaces and interconnected network of pores. In lithologies having gravel and sand particles or fractured rocks such as limestone have large interconnected pore network so water can move through these easily due to porosity and permeability and because of good permeability and porosity these are good aquifers

Water table varies depending upon the several factors such as pumping rate and recharge through precipitation and melting of snow if the pumping of groundwater is higher than recharge rate then groundwater table will fall in subsurface at that place

It is important source of providing fresh water in arid and semiarid areas such as Pakistan because it maintains stream flow even in dry weather

1.3. Importance of water and problems in Pakistan

Most of the largest glaciers of the world are situated in Northern Pakistan. In winter, heavy snowfall occurs in these regions which accumulate over the time and some of which is melted in the summers as runoff for mighty Indus River. This runoff flows from river to canals and other small channels in the lowlands providing irrigation source for around 17 Million hectors of cultivable land which is half of the total cultivable land (34 Million) usable in territory of Pakistan. Glaciers are tremendous gift of nature for this alluvial region. Irrigation system of Pakistan is world's largest system. River Indus and its tributaries Chenab, Jhelum, Ravi and Sutlej rivers provide around 145 MAF during flood period and 105 MAF of this water is faded into the canals. And around 31 MAF of this total water is not used and flows into the Arabian sea which is wasted as it no fresher water. About 8 MAF of water is evaporated or seeped into ground. In Pakistan, Main source of water is Indus River. Canals are constructed for agricultural needs and also major source of groundwater recharge. The other uses of water are Domestic purposes, power generation, drinking etc

1.4. Water Problem:

Increased, imbalance and unfair exploitation of water has lead towards water availability problems in Pakistan, although Pakistan had one of best canal system but due to poor management it is not functional. Annual precipitation is also not contributing towards water availability in this region due to mismanagement of storing and treating rain water for human benefits. Due to Increase in population densities and increase in use of water for agriculture water quality and quantity is greatly affecting negatively.

1.5. Aims and objectives

1. Our objective is to perform quality of water analysis and effects on ground water so that supply of sustainable clean water can be ensure by utilizing our comparative analysis
2. This study can provide a basis to future researchers interested in water quality analysis of surrounding sectors.

3. Concerned study has utilized geophysical approaches such as VES and ERT for getting analysis of leachate and its extent of pollution
4. Our study contains advantages, applications and limitations of approaches such as ERT and VES that can help in future studies regarding discussed approaches

1.6.Introduction of Study Area

1.6.1. Islamabad

It is federal capital of Pakistan located between two provinces Khyber Pakhtunkhwa and Punjab has area of 1,165.50km2 of federal territory and 906.00km2 of urban territory. It is classified in 5 zoneations . Zone I and II are allotted for urban zones . Zones are further subdivided into sectors A - I. They increase north to south from A to I, while sector number increases east to west from 1 to 20. The climate of capital territory is sub-tropical to humid having five seasons spring, summer, rainy monsoon and autumn. The major rivers draining the area are soan and kurang rivers. Islamabad has three artificial reservoirs or dams, which serves as major water recharging sources Simli, khanpur and rawal dam. Northern Islamabad of about 220 acres lies on Margalla hills which is a topographic belt. Margalla hills consists of limestone and shale and in southern part hills derived alluvium deposits, wind derived loess and silt are dominated. Sedimentary deposition sequences are mainly due to indo-oceanic convergence

1.6.2. Location and accessibility

Metropolitan area Islamabad lies between province of Punjab and khyberpakhtoonkhwa having coordinates33.70413704854193, 73.09217610730545 lies on the foot of Margalla hills. Shown in Fig.1. (ii) It is the federal territory of Pakistan having examplery network of interconnected roads of the proper principles of arrangement, ranking and spacing in township road network in grouping with a properhierarchical development of community and central functions. It is connected to the other cities from twin city Rawalpindi. Islamabad is connected to Rawalpindi with faizabad interchange and connected with Lahore and Peshawar via M-2 and M-1.

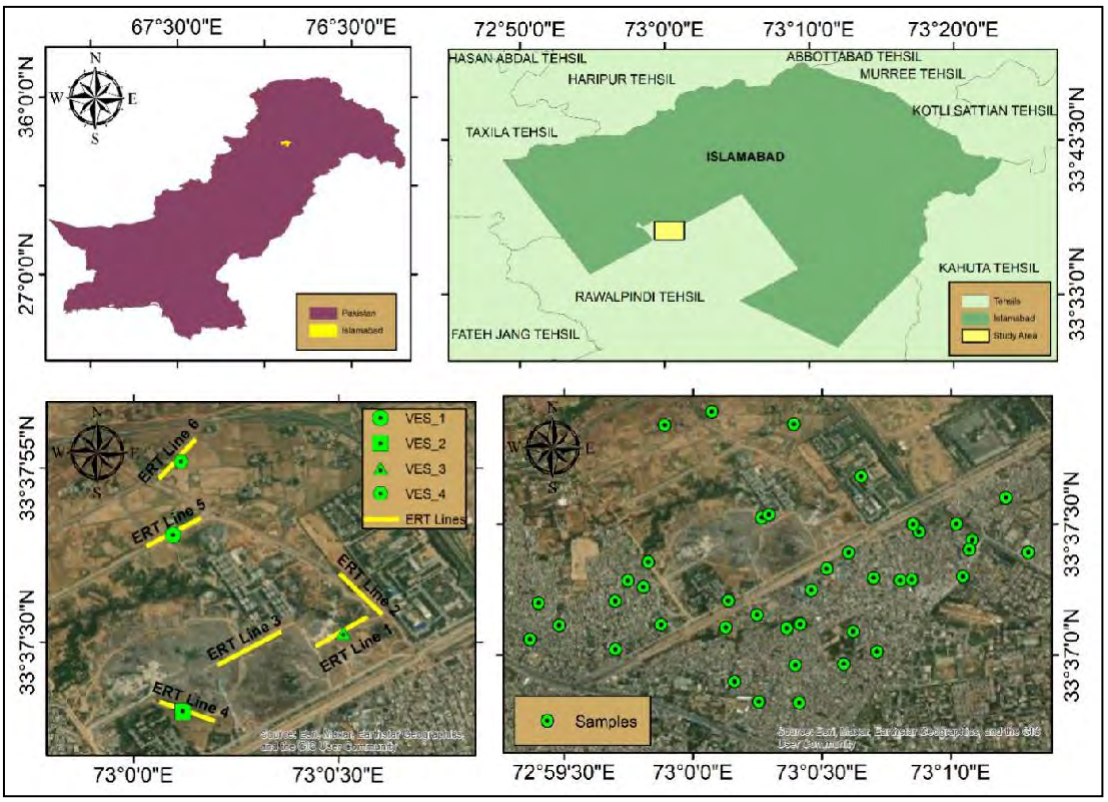

Figure-1.1 Detailed map of district Islamabad along with adjacent areas (ii) location of ERT lines (iii) along with samples location

1.7.Geology and hydrology of Islamabad

Capital territory of Islamabad is located at the foothills of Himalayas, one of the tectonically active zones in the middle of Indo-Pak and Eurasian tectonic plates. series of thrust faults are formed because of collision of two major lithosphere plates Indian and Eurasian plates that had begun 50Ma approximately, older rocks are exposed to surface due to faulting and now can be observed in margalla hills (Sheikh et al.,2008). Islamabad city lies on main boundary thrust (MBT) in hazara Kashmir syntaxis which is active tectonic zone (Waseem et al., 2020). The geology of Islamabad includes exposed jurassic to pliestocene sequence in surrounding of Islamabad younger and older lithologies have inputs such as carbonates and clastics. Environment of deposition is influenced by sea level fluctuations such as older lithology's are deposited in shallow marine environment but as sea level fluctuates The lithology exposed in and its surroundings range in age from the Jurassic to the Pleistocene, with clastic and carbonate deposits occurring at various intervals (zahir, 2020).

The older rocks in the region were formed shallow marine environments, whilst the newer rocks were having deltaic to fluvial depositional environments because of substantial variation (Shah, 2009). In the study region, formations of Mesozoic and Cenozoic have marine depositional environment having thickness of more than 630m while the formations such as Murree, chinji, kamlial and others like Nagri ,dhokpathan , Soan having fluvial environment of deposition having approximately 7000 meters of thickness (Shah (2009) and Khatak et al. (2017It is also worth noting that perhaps the Kuldana Formation has both marine and fluvial elements. however, the alluvium sediments underlying Conglomerate provide a shallower water level, which is most commonly utilized by government and residential wellbores (which are not exactly placed.

According to a 2014 research by Hydro-Geophysical and Environmental Studies Consultants (HESC), the region has five to five groundwater levels. Because of the lithological variety of the studied region, this ground water form may not occur in all places. (Zeeshan, 2020)

1.8.Climate

Climate of Islamabad is sub-tropical humid climate having seasons that are spring, summer, autumn and winter. Spring is quite pleasant lasts from March to April, summer is hot from May to august, then dry and warm autumn lasts September to October then Islamabad experience cold winter from November to February.

1.9.Drainage

Primary streams draining the Islamabad area are soan and Kurang Rivers. Tributary draining northwestward in soan is Ling river Their primary tributaries are the Ling river ; another one is draining westward into the Kurang from the area between the Kurang and Soan is Gumreh Kas; and tributary from mountains and urban area that is draining southward into the Soan is Nala Lei.Supply of water to the urban areas are both of rivers fall into Lakes. Over exploitation of waters and drought has changed the dynamics of water in Islamabad and Rawalpindi

Nala lei tributary is extremely polluted by the domestic and industrial waste declaring it unfit for use of living beings, ground water dynamics are effecting by

seepage of this polluted water. This water infiltrates and become part of ground water at shallow levels which is then exploited by nearby pumped wells (S. MUNIR, 2011)

Sediments found in the region seem to be of strata which range in age from the Cretaceous to the Holocene. The compacted deposits are predominantly formed limestone, sand, kaolin, shale and conglomerate. Such accumulations are not aquifers, and water primarily moves through joints or fractures. Terrace aggregates and alluvial infill are recent poorly compacted depositions. Groundwater is found in alluvial and firm rock beds in the Islamabad region. Consolidated deposits have a relatively limited channel capacity.

As a result, it should only be considered for minor yields in areas where there is a severe public water deficit. However, floodplain aquifer may support massive freshwater exploitation.

Chapter 2 Tectonics and geology

2.1 Regional Tectonic Setting

Geology of Rawalpindi Islamabad is mainly controlled by indo-eurasian convergence which began 20Ma ago caused complex stratigraphy in Islamabad that has been studied by Pakistani as well as foreign geologists

Pakistan having unique distinction, because of its presence at the junction of Indian and Eurasian plate. The ongoing collision between Indian plate and The development of the Himalayas by the Eurasian plate, which is occurring at a pace of 5 mm/year, has resulted in a surprising array of continuous fold-and-thrust structures inside Pakistan Indo-Eurasian lithospheric convergence and collision is the major force regulating the tectonics of the Rawalpindi adjacent Islamabad area, which started around 20 millions of years ago (Kazmi & Jan, 1997).

Islamabad contains valley networks which are consequence of tectonic movements instead of any erosion i.e fluvial or glacial during orogenic periods, the uplifting results in the formation of troughs, the depletion of slopes, fans, and the accumulation of lacustrine sediments. Such deposits are highly coarse and have a higher fluid conductivity

2.2 Structural Setting

The Islamabad-Rawalpindi region may be split into three fundamental sections that exhibit contraction and displacement directed S 20° E

Covering the time period from Jurassic to the Eocene limestone and shale of the upper Margalla Hills in the northwest is complicatedly fractured and pushed all over the faulted line. Orogeny of these mountains most likely resulted in a major topographical barrier (Sheikh and Pasha, 2001). The folded zone is a southern piedmont is covered mostly by termination folds southwest of the Himalayas. In Rawalpindi Group shale and sandstone. The Soan River usually runs all along Soan syncline at the region's southern portion.

2.3 Hazara fold belt

Islamabad is located on the Hazara fault zone's southern boundary and upper end. With the exception of the fault south of Islamabad, all of the faults in the mapping region are members of this fault system. This area comprises of a convex arm of thrusted and deformed strata approximately 25 km broad and 150 km long that stretches west-southwestward from of the Himalayan syntaxis. Throughout the 25-km-wide region northwest of Islamabad, more than 20 separate thrusting layers have been found, however only 5 major thrusts are inside the map region. Several of the fault zone in the Islamabad region are somewhat oblique to one otherAs a result, they extend west-southwestward under the covering of the piedmont folding zone. These faults' expansions are visible to the north of Feteh jang. 25 kilometers west of Rawalpindi, they comprise the south boundary of the Kala Chitta Range, and constitute the en echelon continuation of the Margala Hills three - dimensional framework. The thrust and fold structure of the Margala Hills, immediately north of Islamabad is complex.

2.4 Piedmont fold belt

Although definite exposures are rare and discontinuous, the faulting and folding in the piedmont folding zone southeast of the mountains flank have a strong potential for activity. The Conglomerate of Pleistocene age, which overlies the Murree Formation sandstone (lower Miocene), is deformed in the wide inclined plane near Islamabad's Shakar Parian Park. The Lei Conglomerate is likewise inclined 80 degrees southerly across a fault zone in Kuldana Formation of lower eocene age approximately 17 kilometers northwest of Rawalpindi. The Golra fault might represent an eastern continuation of the southerly over thrusting of the mountainous face all along southern side of Range, a significant range that started approximately 25 kilometres northwest of Islamabad and continues towards Margala Hills. Significant faults that run through the Khalri Murat Range, approximately 15 kilometers south of Range, may also continue northeast into Rawalpindi, hidden behind (Sheikh and Pasha, 2001).

2.4.1 Syncline Soan

The Soan syncline is a regional-scale, asymmetric, faulted fold wherein riverbed sandstone, mudstones, and conglomerate of the Siwalik Formation dip 60°-85° towards the syncline's axis just on northern arm while 45°-70 degrees on the southern limb. The total width of the region in the map region is roughly 12 km, while the fold continues 80 km to the southwest. The greatest breadth is 23 kilometers, located around 30-4 kilometers south of the zone of attention. At least 32km length two protrudes of a northeastern part of thrust fault of the region of interest All along southern extremity, the development is approximately parallel to the folding plane.

Seismic data suggests that the north terminus of the syncline is interbedded at depths by a northward back thrust through an antiformal layering of rock layers, subsequently followed by a convoluted southern faulting (Baker and Lillie, 1989). This type of back thrust is absent from the outcrop, possibly due to region is mostly buried by Quaternary sediments. If such a reading is accurate, the thrust faults beneath the Soan syncline would have carried the bulk of the tectonic contraction along syncline. The external block that holds The syncline might represent a pop-up feature, which would reflect the area's relatively easy deformation. (Wardlaw, 2007) (iqbal M.sheikh, 2007)

2.5 Geological setting

The physiography of Islamabad is made up of plains and mountains with a total relief of more than one meter. The region is situated in the Himalayan foothills and is composed of Tertiary and Pre-Tertiary sediments. It is a component of the Indo Genetic synclynorium. The project area is situated on a low relief surface with Margalla Hills encroaching from the northeast. The rocks in the region are classified as sedimentary and range in age from Jurassic to Recent. The limestone, shale, and sandstone lithology. There are exposed conglomerates, gravels, and clays in the area. These Miocene and earlier rocks have thin alluvium layers covering their upper thin layers. Due to the fact that they make up the majority of the gravel, the primary ground-water aquifer, the gravel and loess are particularly significant to the geology. Due to the increasing complexity of folds and faults in strata caused by its location in a moderate seismo-tectonic hazard zone, their thickness ranges from a few feet to

several hundred feet. In the Islamabad area, this process resulted in complex structure and stratigraphy.

Their thickness varies from few feet to hundreds of feet due to the complex nature of folds and faults in strata due to its location in moderate seismo-tectonic hazard zone. This process produced complex structure and stratigraphy in the Islamabad area (Kadwai, 1966).

2.6 Stratigraphy

The stratigraphy of Islamabad reveals that the area is underlain by sedimentary rocks. Limestone, sandstone, conglomerate, siltstone, and clay of marine and continental origin, with ages ranging from Jurassic to Recent.

2.7 Margalla Hill limestone

The composition is made mostly of limestone with little marl and shale. Grey, weathered bluish gray, finer to moderate grained, granular, moderate to wide, and rarely huge limestone. Marl is gray to brown greyish in colour, while shale is green brownish. The Limestone is approximately 100 metres thick at Shahdara, Both the higher and lower contacts with Patala also Chorgali are conformable .This formation dates from the Early Eocene (Fatimi, 1973 & Shah, 1977).

2.7.1 Murree Formation

The deposit is made up of a repetitive series of darker red and purplish clay, purple grey and greenish grey sandstone, and conglomerate. At the Northern Potwar, the Murree Formation is 303 m thick. Itis unconformably overlain by Eocene Kuldana strata. It has an increasing thickness with upper contact with the Kamlial Formation. Murree Formation dates back to the Miocene (Fatimi, 1973 & Shah, 1977).

2.7.2 Lei Conglomerate

The formation is made up of coarser boulder and pebble conglomerates, as well as small coarser and cross bedded sand (Shah, 1977). Conglomerate is composed primarily of boulders and pebbles derived from Eocene strata, along a tiny amount of grains derived from earlier sedimentary rocks. The gravel of the Lei conglomerate is similar to the Eocene succession of Limestone, that served as the conglomerate's

source (Khawaja & Abbasi, 1983). In the Kohat-Potwar Province, the formation ranges about 150m to 900m approximately (Shah, 1977).

Chapter 3 Review of geophysical methods

A number of geophysical approaches available for detecting "shallow" subsurface features. Resistivity, induction of polarization, electromagnetic techniques, ground probing radar, and magnetometer are the most often utilized. The first four methods are called "active" because they measure the influence of an intentionally manufactured field, whereas magnetometer is considered a "passive" approach since it measures the impact of field. A summary of the approaches and their most prevalent uses are following

3.1 Resistivity method

The fluctuations in the earth's resistivity are determined using this approach. Charges are sent through the earth, and measure the difference at the ground provide an approximate representation of the underlying pattern

3.2 Induced polarization method

This approach is quite identical to the method of resistivity, except it makes advantage of the capacitance generated by conductive substances. It is primarily employed in resource prospecting(Sumner, 2012).

3.3 Electromagnetic methods

The surface is subjected to an oscillatory EM field (primary). This field creates convection in a preexisting conducting body, which subsequently serves as a generator of other electromagnetic field. The ensuing influence of such two positions is measured, and electromagnetic characteristics of the body are acquired in this manner. Electromagnetic techniques are the fundamental approaches for quantitative evaluation of valuable prospects(Ward & Hohmann, 1988).

3.4 Ground Penetrating Radar method

Electric and magnetic frequencies are linked in earth through receiving antenna. They are partially bounced back at any discontinuities of dielectric. The returned

wavelengths are recorded and give data for discontinuity. In civil engineering surveys, radar is often employed(Daniels et al., 1988).

In fact, there isn't one ideal approach that's guaranteed to produce reliable and helpful findings regardless of aim of defining, because each methodology tends to grab some sorts of objectives quicker than others. Additionally, besides the desired features important, but so is the environment. This is due to the major focus in geophysical methods is not always the absolute worth of an intellectual, instead the differential between both the valuation of the feature and the environmental elements

3.5 Electrical Resistivity Method

It is used to investigate the electrical properties of subsurface materials. This method involves the measurement of the electrical resistance of the subsurface materials, which can provide information about the geological and hydrological characteristics of the subsurface.

Principle: resistivity through a medium is defined as the ratio of the electric field strength to the current density. The electrical resistivity of a material is dependent on the type of material, the temperature, and the moisture content(Thiele et al., 2021). In general, resistivity increases with increasing temperature and decreases with increasing moisture content. By measuring the electrical resistivity of subsurface materials, it is possible to infer their moisture content and type (Kearey et al., 2002). Shown in Fig.2.1.

The basic principle of electrical resistivity measurement has been shown in below figure 3.1. In which four electrodes are used which are A,B and M,N.Where M and N is the two potential electrodes and A,B is the two current electrodes.A,B are connected with a battery and ammeter (fig.2.1) that’s used to measure the current and potential difference is measured by a voltmeter between two potential electrodes(Pratt et al., 1988).

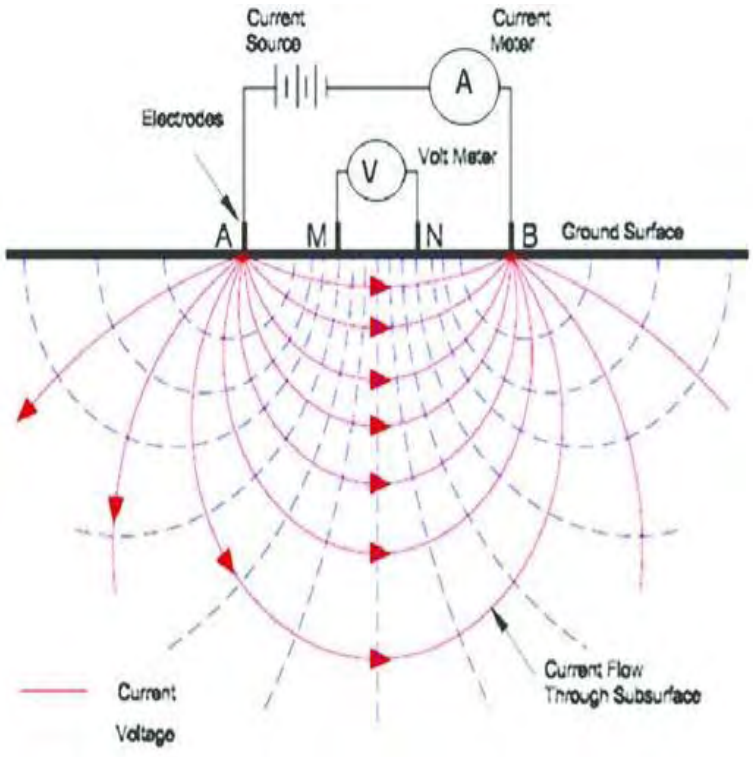

Figure-2.1 Principle of electrical resistivity method

Method: In the electrical resistivity method, electrical current is introduced into the ground using electrodes. The electrodes are placed on the surface or at a depth in the subsurface, and a voltage is applied to the electrodes. The electrical resistance of the subsurface materials is measured between the electrodes. The electrical resistance of the subsurface materials is then used to calculate the electrical resistivity of the subsurface(Shanmugam, 2025).

3.5.1 Flow of current in subsurface

The flow of electrical current in the subsurface is an important technique used for geophysical exploration and environmental monitoring. Understanding the flow of current in subsurface materials can provide valuable information about the subsurface structure, such as the location and extent of subsurface features and the distribution of subsurface materials.

Here are some notes on the flow of current in subsurface through various layers and different scenarios, along with some relevant references:

Homogeneous Subsurface: In a homogeneous subsurface, the flow of electrical current is controlled mainly by the resistivity of the subsurface materials. Current flows from a source electrode to a receiver electrode, and the electrical potential decreases linearly with depth (Safeeq & Fares, 2016). Several studies have utilized electrical resistivity imaging (ERI) to interpret the subsurface resistivity distribution in homogeneous subsurface environments, such as in aquifers.

Layered Subsurface: In a layered subsurface, the electrical properties of each layer can have a significant effect on the flow of current. Current flow can be concentrated in conductive layers or diverted around resistive layers, resulting in complex potential distributions. Researchers have used ERI to investigate the subsurface layering in various applications, such as in geothermal systems and hydrocarbon reservoirs (Heenan et al., 2015).

Anisotropic Subsurface: In an anisotropic subsurface, the electrical properties of the subsurface materials vary in different directions. This can result in a complex flow of current, with different current flow patterns in different directions. Researchers have used various electrical imaging techniques, such as magneto telluric and induced polarization methods, to investigate anisotropic subsurface environments, such as in fractured rock(Binley et al., 2015).

Heterogeneous Subsurface: In a heterogeneous subsurface, the electrical properties of the subsurface materials vary widely in space. This can result in a complex flow of current, with different current flow patterns in different areas. Researchers have used ERI and other electrical imaging techniques to investigate subsurface heterogeneity in various applications, such as in contaminated sites(Ward, 1988)and geological structures(Zohdy et al., 1974).

Dynamic Scenarios: In dynamic scenarios, such as during pumping or infiltration, the subsurface electrical properties can change over time. This can result in changes in the flow of current and the electrical potential distribution. Researchers have

used time-lapse ERI and other time-lapse imaging techniques to monitor changes in the subsurface electrical properties and the flow of current, such as in groundwater pumping (Loke & Barker, 1995) and soil moisture monitoring (Telford et al., 1990).

In conclusion, current flow is a complex process that is influenced by various factors. Electrical imaging techniques, such as ERI and magneto telluric methods, have been widely used to investigate the subsurface electrical properties and the flow of current in various subsurface environments.

Ideally, the optimum geophysical survey should have been a project that employed as several approaches as feasible to capture as much data as feasible. In practice, this is not achievable, hence two (or even one) approaches are typically considered sufficient to generate a decent representation of the subsurface. In comparison to the other approaches, there are several general benefits to resistivity:

- Resistivity survey equipment (Resistivity meter) cost approximately 19 times lower than the instruments employed in many other techniques, making resistivity procedures financially appealing.
- Resistivity measurements are generally straightforward to understand (particularly resistivity profiling) and can provide reasonably reliable subsurface insights even without processing; however, this is only true whenever the characteristics have simple structures.
- Resistivity may reveal a lot across the vertical as well as lateral directions.
- Resistivity is indeed not vulnerable to outside elements such as power lines or metallic debris.

The most important resistivity limits, viewed from the other side, are as follows:

- Complicated structures confound the understanding of resistivity.
- It is not completely nondestructive since probes must be inserted into the prospected region.
- Information gathering can become fairly difficult and lengthy when a significant number of measurements need to be gathered; as a result, it is not easily suitable

to surveys in constructed buildings. Additionally, the technique's absorption is constrained by hardware constraints (length of cable, electrical power).

- It is quiet delicate to shifts in moisture levels of ground, terrain, and variation in surface surface resistivity.

As is clear, resistivity is not the "ideal" approach. Despite its drawbacks, this could produce high-quality data and, in certain situations, give adequate knowledge well about ground without applying other techniques.

3.5.2 Geometric Factor

In the electrical resistivity method, one of the important parameters that affects the measurement of electrical resistivity is the geometric factor. The geometric factor is a measure of the efficiency of the current flow through the subsurface materials, and it is defined as the ratio of the spacing between the electrodes to their diameter. In this chapter, we will discuss the importance of the geometric factor in the electrical resistivity method and how it affects the accuracy of the measurements.

3.5.3 Importance of Geometric Factor

The geometric factor is an important parameter in the electrical resistivity method because it affects the distribution of the electrical current in the subsurface materials. The electrical current introduced into the ground using the electrodes needs to flow through the subsurface materials in order to generate the electric field that is used to measure the electrical resistivity. The efficiency of this current flow is dependent on the geometric factor of the electrode configuration.

If the geometric factor is too large, the current flow will be concentrated at the electrode edges, resulting in a non-uniform distribution of the current in the subsurface materials(Telford et al., 1990). This can lead to inaccurate measurements of the electrical resistivity, as the current flow through the subsurface materials will not be representative of the true electrical properties of the materials. On the other hand, if the geometric factor is too small, the current flow will be too diffuse, leading to a weak electric field and low measurement sensitivity.

3.5.4 Optimization of Geometric Factor

The optimization of the geometric factor is an important consideration in the electrical resistivity method, as it can significantly affect the accuracy of the measurements. The geometric factor can be optimized by choosing an appropriate electrode configuration that takes into account the subsurface characteristics, the depth of the investigation, and the desired resolution of the measurements.

For shallow investigations, a small electrode spacing is preferred in order to increase the measurement sensitivity and resolution. However, for deeper investigations, a larger electrode spacing is needed to ensure that the current flow penetrates deep into the subsurface materials(Telford et al., 1990). The choice of electrode configuration can also affect the measurement sensitivity, with different electrode configurations having different sensitivity to different types of subsurface materials. Resistivity of some rock materials are given in table 1.1

In general, the geometric factor should be optimized to ensure that the current flow is as uniform as possible throughout the subsurface materials, while still maintaining an appropriate level of measurement sensitivity and resolution(Zohdy et al., 1974).

3.6 Conduction of electricity in soil

The resistivity method involves the introduction of direct electrical current into the ground. There are three ways via which the electrical current can be conducted within the earth:

Electrolytic conduction: The flow of electrons travels throughout all the pores of rocks or soil that contain water and charges of soluble minerals and salts. It refers to ions conductivity, which is critical for such resistive approach while most rocks transmit electric charge through such a mechanism.

Ohmic conduction: The propagation of electrical current through the crystal lattice of certain substances, primarily metallic. That type of conductivity, also called electrical conductivity, is critical for mineral prospecting

Dielectric conduction: The presence of an oscillating or AC electrical fields can induce electrons in the lattice of an insulator to conduct. This oscillation can be observed as an ac voltage. In spite of the fact the alternating current is utilized in resistivity potential zones, the frequencies are so low that conductivity of dielectric is typically regarded unimportant.

The resistivity technique's purpose is to quantify the potential changes on the ground caused by flow of current inside the earth. The observed reduction in voltage represents the complexity in causing an electric charge to pass it through ground, providing an indicative of the ground's electrical resistivity p, is directly reliant on how the flow is carried through into the surface. Even though current transmission is connected to underlying geology (ohmic conduction) and ground water (electrolytic conduction), understanding resistance can be used to differentiate preexisting earth characteristics (layering, structures). The formula for the electrical resistivity p of a cylinder with length L and cross section A and resistance R among its terminal sides is

$$\dot{\boldsymbol{\rho}} = \frac{R}{L} (3.1)$$

Where R is measured in ohms, L is measured in meters, and A is measured in sq m. The ohm-meter (m) is the unit of resistivity, p. Permeability, a, is another name for defining the ground's behavior regarding flow of current. It is the inverse of ohm o= 11p and so practically indicates the convenience at which electric charge may be compelled to pass through the ground. Siemens per meter (S/m) is the unit of conductance.

It ought to be noted at this phase that electrolyte conductivity is the most essential factor in determining the earth's resistivity. The variables that impact galvanic conductivity in the subsurface (and hence resistivity) are as follows: According to (McNeil, 1980) and(Tagg) the most important factors are :

a) Water distribution, which itself is affected by weather, time year, and water table depth and soil type.
b) The chemical constituents and quantity of dissolved salts in the water.

c) The particle size of sediments and the porosity of the rocks, as well as any fissures or fractures.
d) Temperatures: Resistivity of earth is heavily dependent on the presence of water, and moisture resistivity is known to be dependent on temperature.

Because the parameters governing electrolytic conduction are so diverse, it is common to see comparable physical configurations manifest as vastly considerable variation in resistivity. As a result, resistivity as a characteristic is extremely volatile, and hence often insufficient, as a technique for extracting precise lithological findings for the underground. While evaluating resistivity data, keep in mind that the observed resistivities really aren't perfect but subjective, and hence only comparative assumptions regarding the rock type of the region can be drawn.

For example, seeing certain data may indicate that a formation is less resistant with respect to the neighboring strata, but it is not feasible to determine its depositional properties just only on the recorded value of resistivity. When this truth is ignored, incorrect interpretations might result.

This limitation cannot rule out effective lithological analyses, but knowledge of the examined region should be addressed in order to produce excellent findings. This preceding information may include geology or geographic information of the region, or data from possible drilling or excavation, or, in fact, any kind of data that might improve understanding of what might be discovered under the ground. This data ought to be collected prior to the measurement Procedure for selecting the best array for resistivity analysis and survey approach.

3.7 2D Arrays

In the electrical resistivity method, arrays of electrodes are used to measure the electrical resistivity of subsurface materials. Different electrode configurations can be used to optimize the measurement sensitivity, resolution, and depth of penetration. Here, we will discuss the different types of electrode arrays used in the electrical resistivity method and their advantages and limitations.

3.7.1 Wenner Array:

The Wenner array is one of the most commonly used electrode arrays in the electrical resistivity method. It consists of four electrodes that are placed in a straight line, with equal spacing between them. The Wenner array is preferred for shallow investigations, as it provides high measurement sensitivity and resolution(Loke & Barker, 1995). However, it has limited depth of penetration, and it is not suitable for deeper investigations.

3.7.2 Schlumberger Array

The Schlumberger array is a popular electrode array for both shallow and deep investigations. It consists of two current electrodes and two potential electrodes that are placed in a straight line, with the distance between the current electrodes being gradually increased. The Schlumberger array provides good depth of penetration and measurement sensitivity, but it has lower resolution than the Wenner array(Telford et al., 1990).

3.7.3 Dipole-Dipole Array

The dipole-dipole array is a commonly used electrode array for deep investigations. It consists of two current electrodes and two potential electrodes that are placed in a straight line, with the distance between the current electrodes being fixed. The distance between the potential electrodes is gradually increased, resulting in a deeper investigation depth. The dipole-dipole array provides good depth of penetration and measurement sensitivity, but it has lower resolution than the Wenner array(Telford et al., 1990).

3.7.4 Pole-Dipole Array

The pole-dipole array is a widely used electrode array for deep investigations. It consists of a current electrode and a potential electrode that are placed in a straight line, with the distance between them being fixed. The potential electrode is then moved along the line, resulting in a deeper investigation depth. The pole-dipole array provides good depth of penetration and measurement sensitivity, but it has lower resolution than the Wenner array.

3.8 Advantages and Limitations of Different Arrays

Each electrode array has its own advantages and limitations, and the choice of array depends on the specific subsurface characteristics, the depth of investigation, and the desired measurement sensitivity and resolution. The Wenner array is preferred for shallow investigations because of its high measurement sensitivity and resolution, while the dipole-dipole and pole-dipole arrays are preferred for deep investigations because of their good depth of penetration (Zohdy et al., 1974).

The Schlumberger array is a versatile array that can be used for both shallow and deep investigations, but it has lower resolution than the Wenner array(Telford et al., 1990). It is important to note that the optimization of the electrode array should take into account the specific subsurface characteristics, as different electrode arrays have different sensitivity to different types of subsurface materials (Zohdy et al., 1974).

3.8.1 Vertical Electrical Sounding

Vertical Electrical Sounding (VES) is a geophysical method used to determine the electrical resistivity of the subsurface materials with depth. This technique is based on the measurement of the potential difference between two electrodes while a known current is passed through the ground. The method can provide a resistivity-depth profile, which can be interpreted to give information on the subsurface geology. The VES method can be used for mineral exploration, groundwater investigations, and geotechnical engineering.

There are three modes of VES measurements: Schlumberger, Wenner, and Pole-Dipole. Each of these methods has its own advantages and disadvantages, and the choice of the method depends on the purpose of the investigation and the geological setting of the site.

3.8.2 1D Schlumberger Method:

The Schlumberger method is the most commonly used VES technique. It involves the use of a current electrode and a potential electrode that are placed on the surface of the earth. The distance between the electrodes is gradually increased, and the potential difference is measured at each interval. The Schlumberger method is preferred in areas

where the subsurface resistivity is expected to vary over a wide range of depths, and the depth of the target is not known(Loke & Barker, 1995).

3.8.3 1D Wenner Method:

The Wenner method is another VES technique that is used to determine the resistivity-depth profile of the subsurface materials. The method involves the use of four electrodes, which are placed in a straight line along the surface of the earth. The current is passed through the outer electrodes, and the potential difference is measured between the inner electrodes. The Wenner method is preferred in areas where the subsurface resistivity is expected to be relatively uniform, and the depth of the target is known (Parasnis, 2012).

3.8.4 1D Pole-Dipole Method:

The Pole-Dipole method is the most sensitive of the three VES techniques. It involves the use of a current electrode and a potential electrode, which are placed on the surface of the earth. Several other electrodes are placed along the surface of the earth at increasing distances from the current electrode (Parasnis, 2012). The potential difference is measured between the potential electrode and each of the other electrodes. The Pole-Dipole method is preferred in areas where the subsurface resistivity is expected to be highly variable.

The choice of VES method depends on the objectives of the study, the geological setting, and the available equipment(Telford et al., 1990). A detailed interpretation of the resistivity-depth profile obtained from the VES measurements is required to infer the geological structures and the potential for groundwater or mineral resources. The VES method is a useful tool in geophysical exploration and has been used successfully in many studies around the world.

The Schlumberger array is a widely used configuration for Vertical Electrical Sounding (VES) surveys because it has several advantages over other arrays. Here are a few reasons why the Schlumberger array is preferred for VES:

Wide depth of investigation: The Schlumberger array is designed to measure the resistivity of the subsurface materials at varying depths. By increasing the distance

between the current and potential electrodes, the Schlumberger array can provide data from shallow to deep resistivity values.

Good resolution: The Schlumberger array has good depth resolution and is capable of detecting small changes in resistivity with depth. This is particularly useful for geological investigations, as it allows for the identification of different layers of rock or soil and the estimation of their thickness.

Minimal noise: The Schlumberger array is relatively immune to noise interference from nearby power lines and other sources of electromagnetic interference. This is because the array measures the potential difference between two electrodes that are placed in the same location, and the measurements are therefore not influenced by external sources of electromagnetic noise.

Fast and efficient: The Schlumberger array is easy to set up and can provide measurements quickly and efficiently. The array requires only two electrodes, which can be moved along the survey line to obtain data at different depths.

Versatile: The Schlumberger array can be used in a wide range of geological settings, from areas with relatively uniform subsurface materials to areas with highly variable subsurface resistivity.

Overall, the Schlumberger array is a popular choice for VES surveys due to its wide depth of investigation, good resolution, minimal noise, efficiency, and versatility.

3.9 Constant Spacing Traversing

Constant Spacing Traversing (CST) is an electrical resistivity tomography (ERT) technique that provides a continuous profile of subsurface resistivity distribution along a straight survey line. The method involves placing a set of four electrodes in a straight line along the survey line and moving them along the line at a fixed interval. The method provides a continuous resistivity profile along the survey line, making it useful for geologic and hydro geologic investigations (Dahlin & Zhou, 2004).

CST is a relatively simple and inexpensive method that does not require specialized equipment. It is also less affected by near-surface lateral heterogeneities and topography compared to other ERT methods(Daily & Owen, 1991). The CST method is commonly used for a range of applications such as groundwater exploration, mineral exploration, and geotechnical investigations.

There are several modes of CST measurements, including the Wenner array, Schlumberger array, and dipole-dipole array. The Wenner array is the most commonly used array in CST measurements. It involves placing the electrodes at equal intervals along the survey line and injecting a current between the outermost electrodes. The potential difference between the two inner electrodes is then measured to obtain the subsurface resistivity. The Wenner array is preferred in areas with relatively uniform resistivity, such as groundwater exploration or environmental studies.

The choice of CST array depends on the purpose of the investigation and the geological setting of the site(Daily & Owen, 1991). The Wenner array is preferred in areas with relatively uniform resistivity, the Schlumberger array is preferred in areas with highly variable resistivity, and the dipole-dipole array is preferred in areas with highly variable resistivity.

3.10 Applications

There are several instances of effective applications of the resistivity approach to a wide range of subterranean issues in the literature. The following are the most prevalent resistivity applications:

Geological Mapping of the earth's interior have frequently employed resistivity(Griffiths & Barker, 1993)

Hydrogeological It is most likely the most prevalent utilization of the resistive approach. Hydro - geological modeling and subsurface water investigation have both made usage resistivity (Olayinka & Barker, 1990).

Geothermal has been successfully used in geothermal field exploration (Thanassoulas et al., 1987).

Engineering has been applied to a wide range of technical hurdles, including dam stability and stability, cavities identification, infrastructure design, and measuring the hydrologic and anisotropic characteristics of the ground (Habberjam, 1975).

Environmental Many uses of resistivity in environmental issues were noted, including identifying ground-water contamination (Rogers & Kean, 1980), litter managing(Barker, 1992)and assessing contamination leaks(Van et al., 1992) etc.

Archaeological resistivity has become the most widely employed technique in archaeometry, and it has been employed for years to find a wide range of ancient finds (Aitken, 1974).

Chapter 4 Methodology

4.1 Survey Design

The groundwater flow is generally from north to south in Islamabad, with the Margalla Hills acting as the primary source of groundwater recharge (Khan et al., 2015).

In order to investigate contamination, I decided to acquire 2 ERT profiles at upstream (North of waste site), 1 ERT profile at downstream (South of waste site) and 1 ERT profile with in waste site in direction which is perpendicular to groundwater flow (North-south). We also placed 1 ERT profile in East of waste site in North-south direction and another ERT profile in South-west of waste site in a Northwest-southeast direction, to investigate flow of contaminations in these directions as shown in figure 4.

I decided to acquire VES data to correlate it with ERT profiles and decided to acquire VES points as 2 VES points at Upstream and 2 VES points at downstream as shown in figure 4.

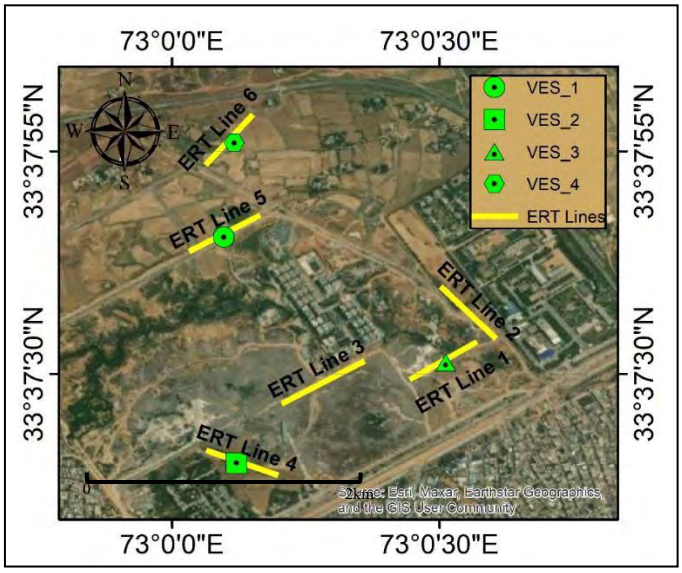

Figure-4.1 Showing ERT profiles with directions

To investigate groundwater contamination cause by waste site, I decided to collect groundwater samples from all directions of waste site. 26 samples in south of waste site,

9 samples in west of waste site, 2 samples in east of waste site, 2 samples in north of waste site and 2 samples from waste site as shown in fig 5

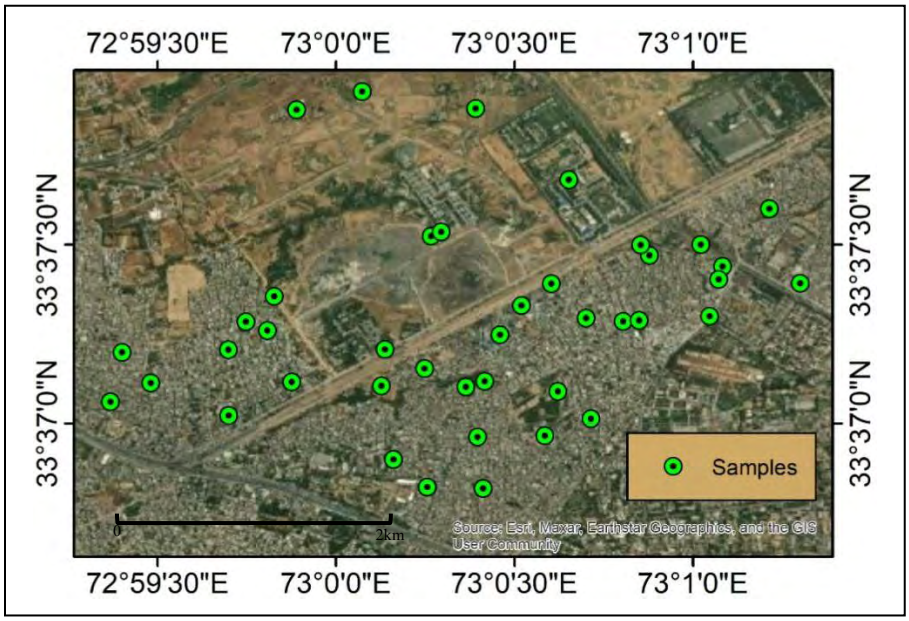

Figure-4.2 Showing Samples locations marked in study area

4.2 Materials

- **Instrument and accessories**

The instruments used in the ERT survey are:

- **Syscal Junior**

It is resistivity and induced polarization sounding and profiling system for environmental claims. The system is brought as a usual sounding system capable of recording two measurements separately, perfect for performing offset Wenner sounding arrays. The output current is automatically adjusted (automatic ranging) to optimize the input voltage values and to certify the better measurement quality. Compact, easy-to-use and field proof, the Syscal Junior measures both resistivity and chargeability (IP). With a maximum power output of 100W at 800Vpp, the Syscal Junior is suitable for most near surface geophysical prospection applications, such as pollution monitoring and mapping, salinity control, depth-to-rock determination, and weathered bedrock mapping.

Figure-4.3 Showing Syscal junior

- **Electrodes**

These are metal stakes with a hole at the top to connect the wires.

48 electrodes are used to carry out this survey because SYSCAL Junior supports only 48 electrodes.

- **Hammer**

4 to 5 small hammers for short electrodes and a heavy sledgehammer for long electrodes.

- **Set of wires**

ERT: Two sets of wires are used (240 meters) with 5 meters interval to connect the all 48 electrodes.

4.3 Field Procedure

4.3.1 Electrical Resistivity Tomography:

It is a geophysical technique to investigate subsurface regime by measuring their electrical resistivity. To acquire ERT data, you will need the following equipment and steps:

Equipment:

- Syscal Junior: This is a specialized device that sends electrical current into the ground and measures the voltage response at different electrode pairs. Shown in fig 6.
- Electrodes: These are metal rods that are inserted into the ground at specific intervals and connected to the ERT instrument via cables.

Steps:

1. Determine the survey area: You need to determine the area to be surveyed and mark the positions where electrodes will be inserted.
2. Set up the ERT instrument: Place the ERT instrument near the survey area and connect it to the electrodes.
3. Connect the electrodes: The electrodes are connected in pairs, with one electrode acting as the current source and the other as the voltage measurement point.
4. Choose “multi-mode “and Select electrode configuration (Dipole Dipole or Wenner schlumberger in this case).
5. Apply RS check from instrument: The ERT instrument applies an electrical current to the ground through the current electrode and voltage response is measured at each electrode pair by the ERT instrument to make sure that all electrodes are connected or not. This process may take about 30 to 40 minutes depending upon the type of electrode configuration and the number of electrodes that are used in the survey.

6. Repeat steps 5: The current electrode is moved to different locations, and the voltage response is measured at each electrode pair again.

7. Collect data: Start the acquisition just by pressing the button “Start”.

4.3.2 Vertical Electrical Sounding:

1. Determine the survey area: You need to determine the area to be surveyed and mark the middle point for VES data.

2. Connect the electrodes: The electrodes are connected in pairs, with one electrode acting as the current source and the other as the voltage measurement point. In our case, we used schlumberger array.

3. Choose “rho-mode” and Select electrode configuration (Schlumberger VES in this case).

4. Collect data: Start the acquisition just by pressing the button “Start”.

5. Repeat the procedure by symmetrically increasing the spread length by keeping the midpoint same.

4.3.3 Collecting Samples for Physio-chemical Analysis

Collecting groundwater samples for physio-chemical analysis requires proper techniques to prevent contamination and to ensure that the samples represent the actual groundwater conditions. The steps involved in collecting groundwater samples for minor and major elements are as follows:

Equipment and tools needed:

- Clean and sterile sampling bottles with caps (one for minor elements and the other for major elements).
- A clean plastic or stainless-steel bailer or a pump with tubing for collecting samples.
- Disposable gloves to avoid skin contact.

- A marker pen to label the sampling bottles.

2. Site selection: Select the location where the groundwater sample needs to be collected. The location should be representative of the area being investigated and should be accessible.

3. Sampling procedure:

    i. Wear disposable gloves to avoid skin contact with the sampling equipment.
    ii. Remove the cap of the sampling bottle and keep it aside without touching the inside of the cap or bottle.
    iii. Using a bailer or a pump with tubing, collect the groundwater sample.
    iv. Transfer the sample into the sampling bottle, filling it up to the top.
    v. Cap the bottle tightly, ensuring that no air bubbles remain in the sample.
    vi. Collect another sample from same location and put nitric acid in it according to the ratio of 10 ml for 1 liter.
    vii. Label the bottle with the site name, location, date, and time of collection.
    viii. Repeat the above steps to collect another groundwater sample in the other sampling bottle.

4.3.4 Processing

Processing of VES is carried out in IPI2WIN software.

Processing of ERT is carried out via two software, PROSYS 2 and RES2DINV.

- **POSYS 2**

Prosys 2 Is Used to Removed Abnormal Resistivity Values to export file with ".DAT" extension to be readable for RES2DINV. Removal Of Resistivity Values Is Based On Standard Deviation, Resistivity Values Having Standard Deviation Greater Than Or Equal To 25 Will Be Removed.

- **RES2DINV**

Inversion in RES2DINV is carried out with following settings

- Robust Model Constraint

Robust model constraint is used for data that is acquired in area having sharp lithological boundaries.

- Robust Data Constraint

One can select the standard least-squares constriction that challenges to diminish the square of the difference amid the observed and calculated apparent resistivity values, or a robust constraint that is least sensitive to very noisy extremities but may provide an apparent resistivity RMS error. My data lacks nois, so, I utilized Robust Data Constraint

- Type Of Method For Least Square Inversion

There are two methods for least square inversion, Standard Gauss Newton Method and Incomplete Gauss Newton Method. Incomplete Gauss Newton Method is used for data having data points more than 3000. So, I used Standard Gauss Newton Method. Remaining filters were used on their default settings.

Chapter 5 Geoelectrical data processing and interpretation

5.1 The ERT line 1 and VES 3

The 2D ERT profiles with 1D VES data

We acquired 6 ERT profiles and 4 VES Points as shown in figure 5.1

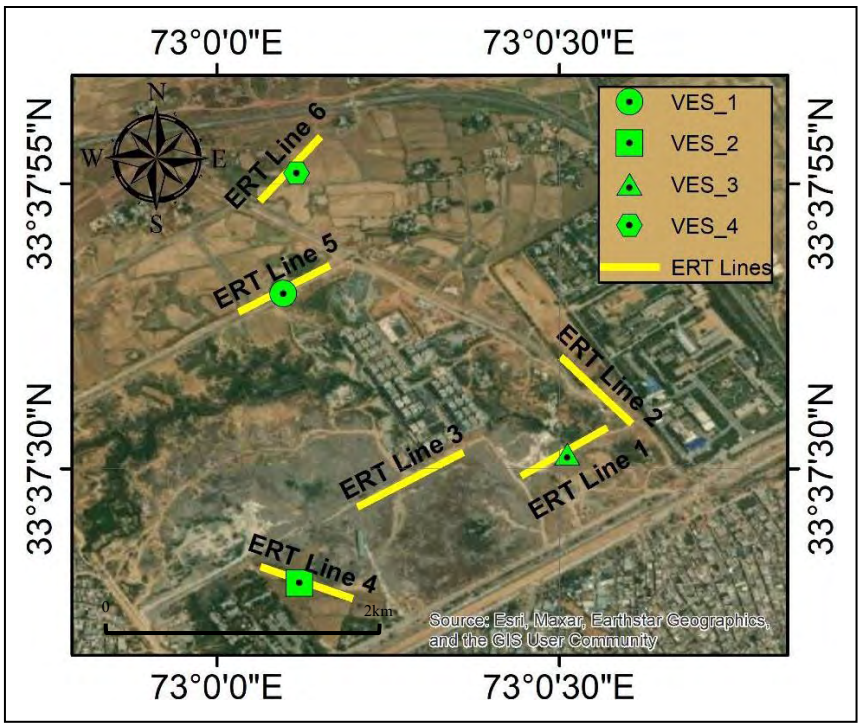

Figure-5.1 Showing ERT and VES points

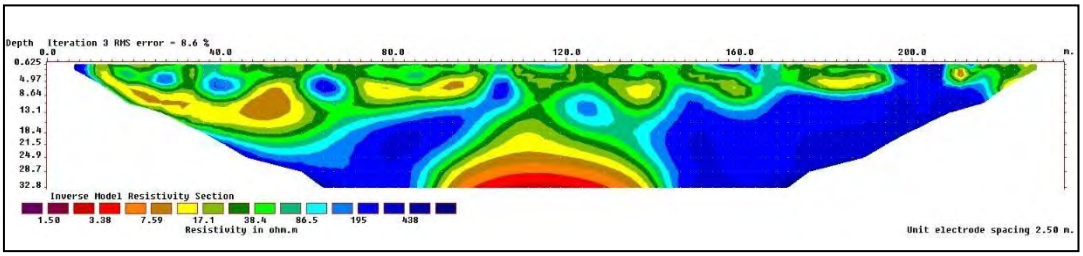

Figure-5.2 Showing Inversion results of ERT Line 1

ERT pseudo section and VES apparent resistivity interpretation

ERT line 1 was performed with Dipole-Dipole configuration. In north of line 1, waste is placed in a depression that is 13 meters below from line 1 elevation. In south of ERT line 1, waste is 5 meters away from central part of line 1 while western (right side of line) and eastern (left side of line) are in direct contact with waste. Inversion results of ERT line 1 are shown in figure 5.2

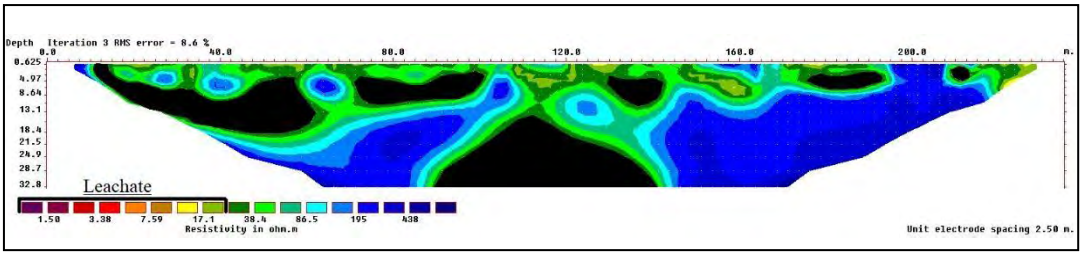

Figure-5.3 Showing Interpretation of ERT Line 1

Contamination plumes can be seen with resistivity of less than or equal to 30 Ωm and shown as black color in figure 5.3 with increasing depth the resistivity of leachate is decreasing as shown in figure 5.3. In central part (at 110m), the leachate can be seen at depth 13.5m while on eastern (130m to 145m, 175m to 195m and 208m to 212.5) and western side (70m to 102.5m and 10m to 62.5m) leachate is near surface.

On western side of line 1, below 10m leachate can be seen percolating into the surface and reaches the depth of 18.4m below 62.5m. Between 70m to 102.5m, leachate can be seen at 2.8m depth and reaches the total depth of 11m.

On eastern side of ERT line 1, leachate between 130m to 145m and 175m to 195m, can be seen from average depth of 2.8m depth from surface and reaches to the maximum depth of 11m while leachate between 208m to 212.5 can be seen from surface and reaches to the depth of 4.9m.

As stated above, waste material is dumped 13m below central point of line 1 and results shows that leachate is started from the depth of 13.5m below 110m. Eastern and

western sides of ERT line 1 are in direct contact with waste material and results are showing that on eastern and western sides, the leachate is near to surface.

VES 3 is acquired at 80m of ERT line 1 and resistivity of 29.1 Ωm has been observed at AB/2 of 15m and resistivity of 31.3 Ωm has been observed at AB/2 of 10m, showing that leachate plume is started between 10m and 15m supporting our line 1 results of leachate starting from 13.5m as shown in table 5.1. Lowest resistivity of leachate is observed in line 1 is at depth of 32.8m and lowest resistivity in VES 3 is observed at 30m and at 35m it started to increase, thus, supporting our ERT line 1 data.

When correlating ERT line 1 with VES 3, we observed that in our study area the depth of penetration of vertical electrical sounding data is equal to the half of the total spread length. investigated in VES 3 in 9.32m in which resistivity values are ranging from 29.1Ωm to 7.16Ωm, curve which is interpreted here in fig… shows varying resistivity and thickness in which upper layer has thickness of 3.46m and resistivity value of 29.1 and lower layer has thickness of 5.86m resistivity value of 7.16Ωm, clearly demonstrated that upper layer has higher resistivity value comparatively

Table-5.1 Showing potential and current electrodes spacing and respective resistivity of VES 3

AB/2	MN/2	Resistivity (Ωm)
2	0.5	31.057714
4	0.5	30.763137
5	1	31.18073
10	1	31.436674
10	2	31.302857
15	2	29.150673
20	2	27.195459
25	2	26.879273
25	5	28.156015

30	5	11.134319
35	5	25.701219
40	5	25.591708
45	5	21.475875
50	5	24.580463
50	10	24.064832
60	10	22.916667
70	10	23.179861
80	10	82.52459
100	10	188.68173

VES true resistivity interpretation:

Total depth which was investigated in VES 3 in 9.32m in which resistivity values are ranging from 29.1Ωm to 7.16Ωm, curve which is interpreted here in fig 5.4 shows varying resistivity and thickness in which upper layer has thickness of 3.46m and resistivity value of 29.1 and lower layer has thickness of 5.86m resistivity value of 7.16Ωm, clearly demonstrated that upper layer has higher resistivity value comparatively

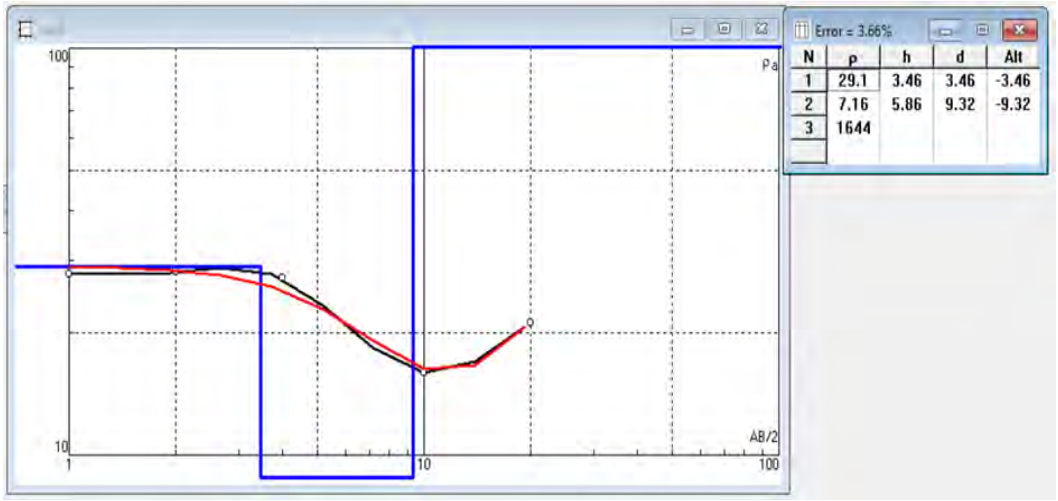

Figure-5.4: Showing layering model for VES 3.

5.2 The ERT line 2

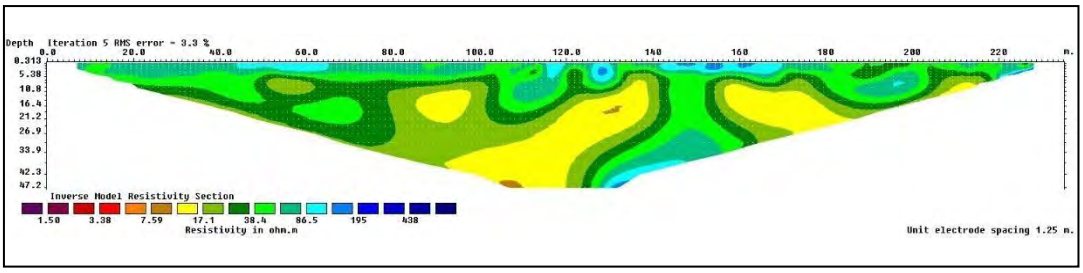

Figure-5.5 Showing inversion results ERT line 2

ERT line 2 was performed with Wenner Schlumberger configuration. ERT line 2 is acquired in east of waste site and in northwest-southeast direction. This ERT line is acquired 125meters away from waste site. Inversion result of ERT line 2 is shown in figure 5.5.

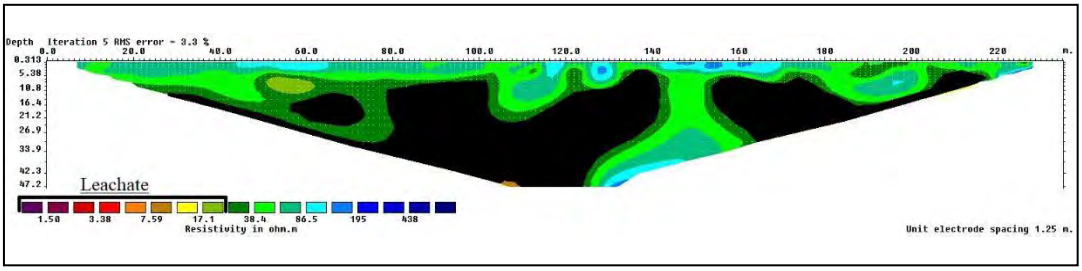

Figure 5.6 Showing interpretation of ERT line 2

Leachate can be seen in ERT line 2 from 28m to 142m at various depths, the maximum observed is 47.2m below 120m and minimum depth is 5.38m below 137.5m while leachate can also be seen from 35m to 143m at various depths, the maximum observed is 47.2m below 120m and minimum depth is 5.38m below 137.5m. Between 163.5m and 217.5m, leachate is observed at various depths the minimum depth of leachate is 5m below 211.25m as shown in figure 5.6.

5.3 The ERT line 3

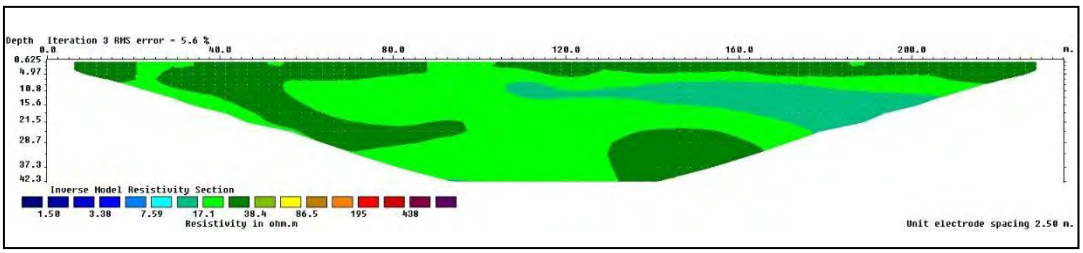

Figure-5.7 Showing inversion results of ERT line 3

ERT line 3 was performed with Wenner Schlumberger configuration. ERT line 3 is acquired within waste site, in east-west direction. This profile is acquired along dumped waste. Inversion result of ERT line 3 is shown in figure 5.7.

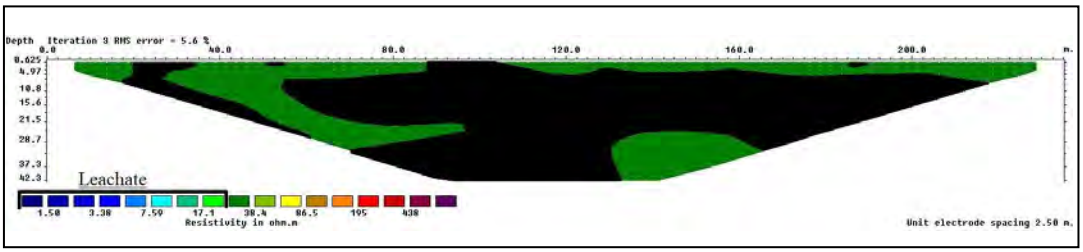

Figure-5.8 Showing interpretation of ERT line 3

In figure 5.8 leachate of resistivity less than or equal to 30Ωm can be seen mostly near the surface while leachate is in contact with surface at 28m to 35m, 87.5m to 102.5m and 185m to 195m. Maximum depth of leachate is is more than 42.3m below the ground surface. ERT line 3 is acquired adjacent to dumped waste, thus, showing leachate near the surface.

5.4 The ERT line 4 and VES 2

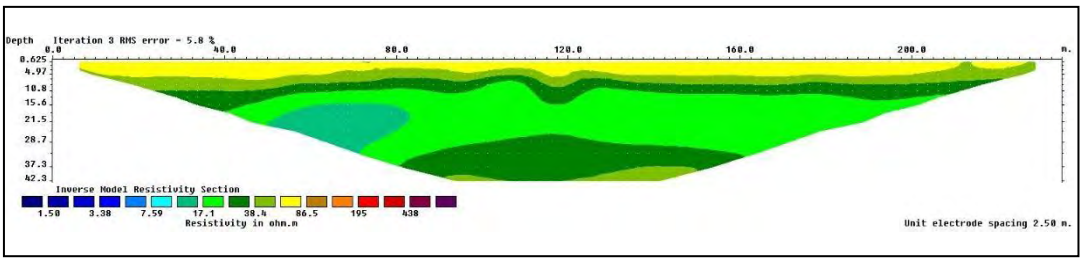

Figure-5.9 Showing inversion results of ERT line 4

ERT line 4 was performed with Wenner Schlumberger configuration. ERT line 4 is acquired in southwest of waste site and in southeast-northwest direction. Southeastern (left) side of profile was much closer to dumped waste and northwestern (right) side.

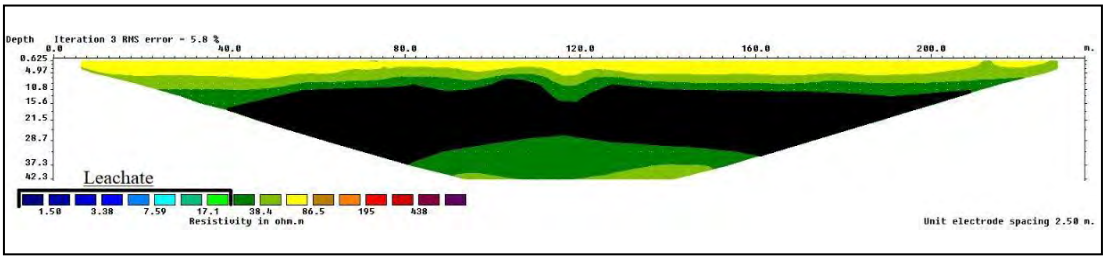

Figure-5.10 Showing interpretation of ERT line 4

In figure 5.10, leachate of resistivity less than or equal to 30Ωm can be seen at average depth of 10m below surface. Maximum depth of leachte bottom is 37.3m at 80m below the ground surface.

VES 2 is acquired at 92.5m of ERT line 4. In VES 2, leachate is observed at AB/2 of 15m with resistivity of 29.28 Ωm which is supported by ERT line 4 in which the leachate can be seen at approximately 15m below 120m. The maximum depth to which leachate is present at 120m is approximately 27m depth which is again supported by VES2 in which the leachate is observed till AB/2 of 25m with resistivity of 27.45 Ωm and at AB/2 of 30m the resistivity observed is 31.01 Ωm, thus, showing that leachate infiltration is ended between 25m and 30m as shown in table 5.2.

Table-5.2 Showing potential and current electrodes and obtained resistivity of VES 2

AB/2	MN/2	Resistivity (Ωm)
2	0.5	75.85201
4	0.5	71.964158
5	1	70.06087
10	1	60.880157
10	2	64.890377
15	2	29.286034
20	2	28.349051
25	2	27.874126
25	5	27.458303
30	5	31.013606
35	5	32.129468
40	5	33.176208
45	5	33.887605
50	5	33.958611
50	10	34.869159
60	10	34.736842
70	10	38.018503
80	10	45.590612
100	10	59.705558

VES true resistivity interpretation:

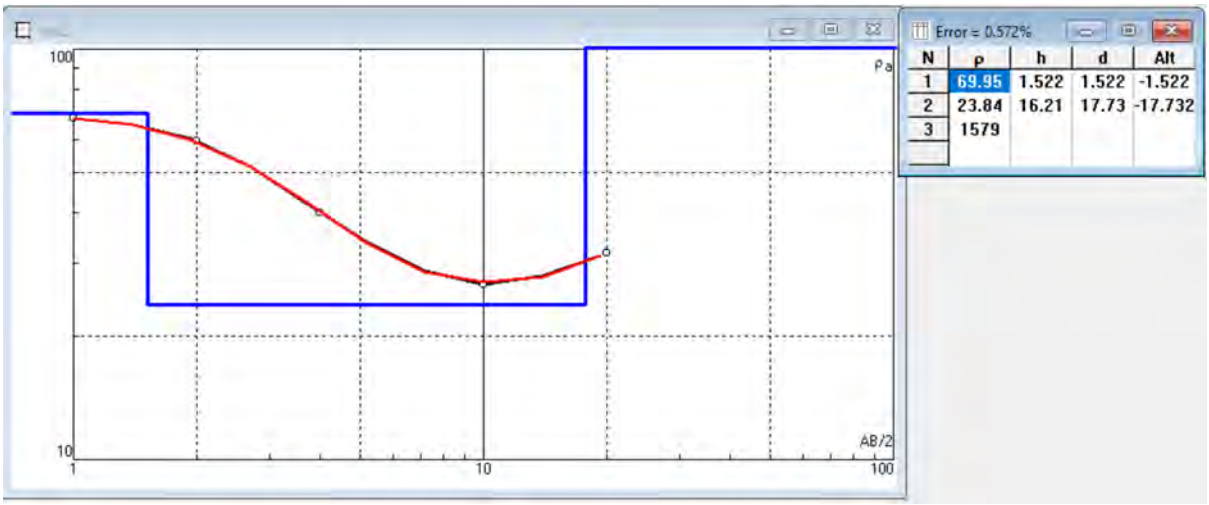

Figure-5.11: Showing layering model for VES 2.

Total depth that is investigated in VES 2 is 17.73m and resistivity is varying between 23.84Ωm to 69.95Ωm and the curve which is interpreted in fig 5.11 .is showing changing resistivity and thickness, thickness of upper layer is 1.522m and resistivity is 69.95Ωm and thickness of lower layer is 16.21m and resistivity is 23.84Ωm, upper layer has higher resistivity value than lower layer.

5.5 The ERT line 5 and VES 1

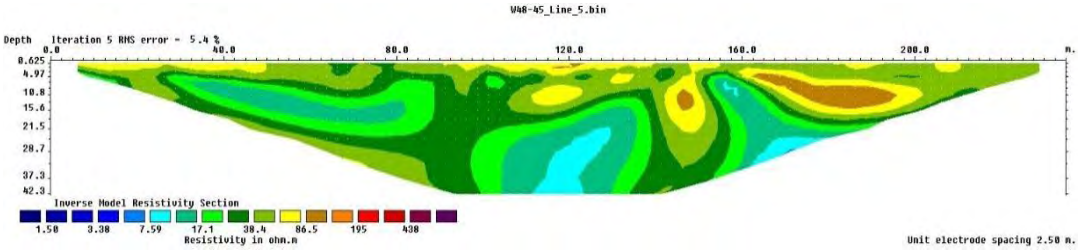

Figure-5.12 Showing inversion results of ERT line 5

ERT line 5 pseudo section and VES apparent resistivity interpretation:

ERT line 5 was performed with Wenner Schlumberger configuration. ERT line 5 is acquired in north of waste site in east-west direction. This profile is acquired at upstream relative to the waste site but it still shows resistivity of less than or equal to 30 Ωm as shown in figure 5.13 by black color in figure 5.13.

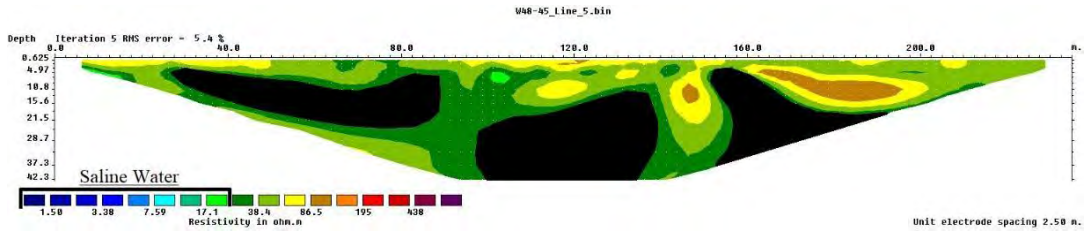

Figure-5.13 Showing interpretation of ERT line 5

This low resistivity is due to presence of waster ponds in the north of ERT line 5 which is the upstream for ERT line 5. Surface water has low resistivity values than groundwater because dissolved ions (Kelly, 2013). Thus, being acquired at downstream of saline water, this profile shows low resistivity values but part of profile which is not in front of ponds is showing resistivity values higher than 30 Ωm which is supported by VES 1. VES 1 is acquired at 92.5m of profile 5 and showing no sign of contamination as shown in table 5.3.

Table-5.3 Showing current and potential electrodes and obtained resistivity of VES 1

AB/2	MN/2	Resistivity (Ωm)
2	0.5	128.4113
4	0.5	90.1261
5	1	73.35334
10	1	48.53911
10	2	45.87097
15	2	39.13923
20	2	36.83284
25	2	34.90033
25	5	35.67111
30	5	34.87908
35	5	33.50779
40	5	32.51433
45	5	31.66341
50	5	31.13627
50	10	31.8633
60	10	31.67909
70	10	32.06561
80	10	32.98685
100	10	40.922

VES true resistivity interpretation:

N	ρ	h	d	Alt
1	69.95	1.522	1.522	-1.522
2	23.84	16.21	17.73	-17.732
3	1579			

Figure-5.14 Showing the layer model that is created through IPI2WIN

Depth investigated altogether at VES 1 is about 63.9 meter possessing resistivity values of 21.1Ωm to 141 Ωm, and curve that is interpreted in figure 5.15 Is showing varying resistivity and thickness in which upper layer has thickness of 1.89m and resistivity is 141Ωm and lower layer has thickness of 45.6m has resistivity is 21.3Ωm which is relatively thicker then upper layer and resistivity value of upper layer is greater than the lower one as shown in Figure 5.15.

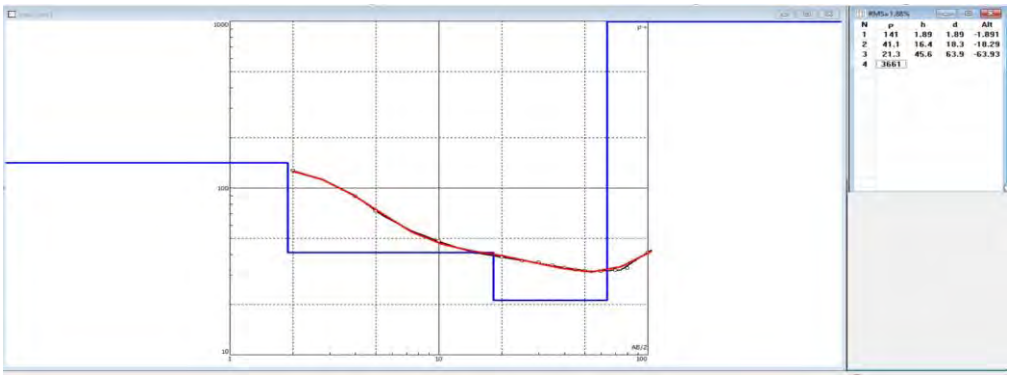

Figure-5.15 Showing layering model for VES 1.

5.6 The ERT line 6 and VES 4

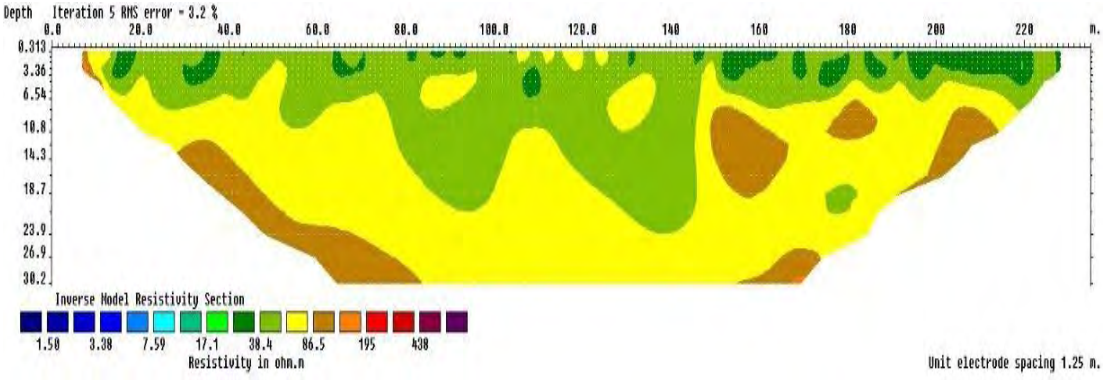

Figure-5.16 Showing inversion results of ERT line 6

ERT line 6 pseudo section and VES 4 apparent resistivity interpretation:

ERT line 6 was performed with Wenner Schlumberger configuration. ERT profile 6 is acquired in north of waste site in northeast-southwest. Inversion result is shown in figure 5.16. This profile is acquired at upstream relative to the waste site. Resistivity values of equal to or less than 30 Ωm are not present in the section, thus, showing no sign of contamination or leachate in this area. A result of ERT line 6 are supported by the VES 4 which is acquired at 82.5m of ERT line 6 is showing no sign of any contamination or leachate as shown in table 5.4. Thus, no leachate is present at the upstream of waste site.

Table-5.4 Showing current and potential electrodes spacing and obtained resistivity of VES 4

AB/2	MN/2	Resistivity (Ωm)
5	1	50.05390514
10	1	48.98530741
10	2	49.64783369
15	2	50.11330833
20	2	52.50067887
25	2	53.99121444
25	5	52.82733781
30	5	55.30422881
35	5	57.01184968
40	5	60.52360226
45	5	63.31240554
50	5	65.43408918
50	10	65.72287183
60	10	69.87802328
70	10	74.14699464
80	10	75.61505915
100	10	80.23004963

VES true resistivity interpretation of VES 4:

N	ρ	h	d	Alt
1	49.4	2.8	2.8	-2.8
2	77.7	6.73	9.53	-9.53
3	79.7			

Figure-5.17 Showing true resistivity interpretation of VES 4

Total depth investigated in VES 4 is 9.53m. Resistivity values in VES 4 ranges from 49.4Ωm to 77.7Ωm. The curve that is interpreted in fig 5.17 showing varying thickness and resistivity values. Upper laying is 2.8m thick having resistivity 49.4Ωm and lower layer is 6.73m thick having resistivity of 77.7Ωm. Clearly demonstrated that upper layer has lower resistivity value that lower layer

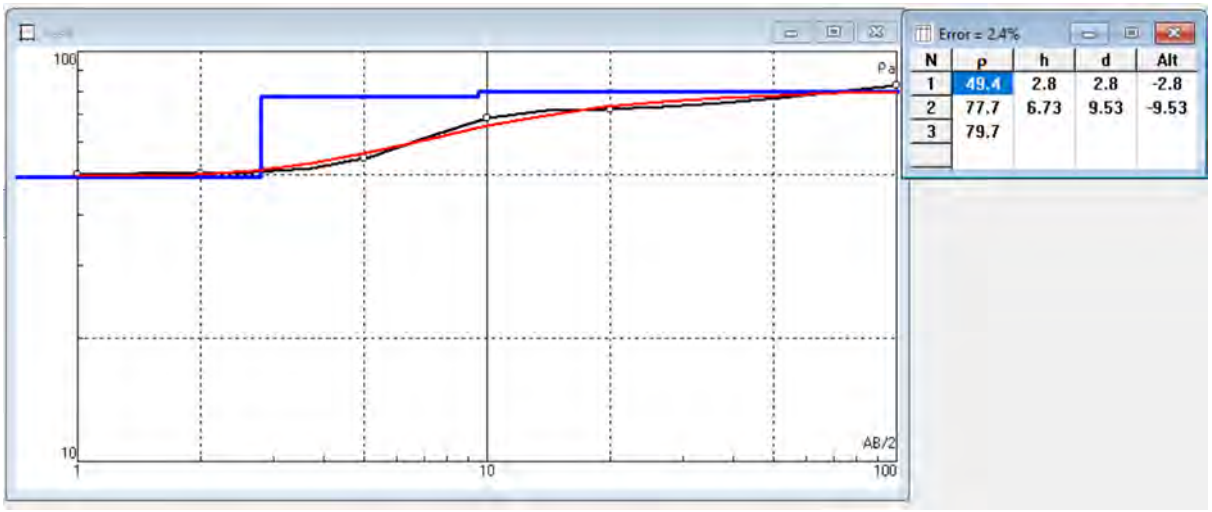

Figure-5.18 Showing layering model of VES 4.

5.7 Correlations between ERT and VES

Correlation between ERT line 1 and VES 3

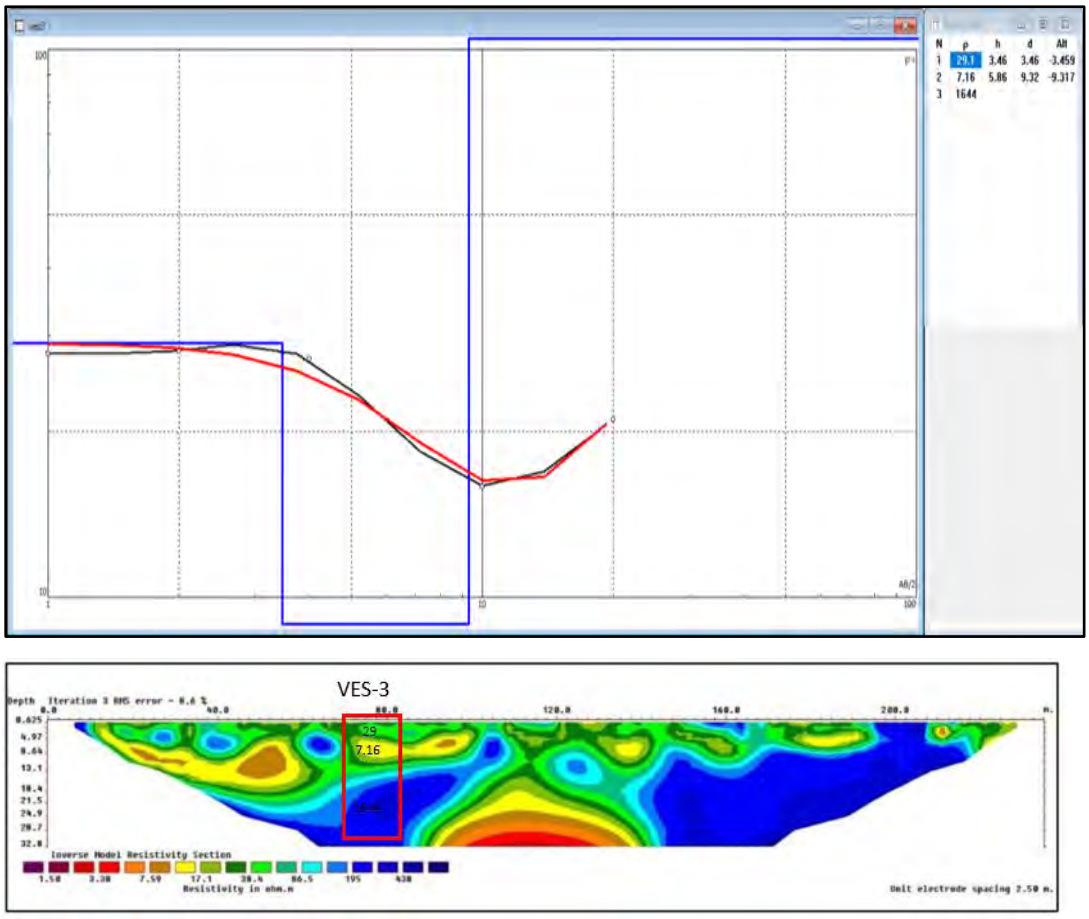

Figure-5.19 Showing correlation between ERT line 1 and VES 3.

Investigated depth in VES 3 in 9.32m have resistivity values are ranging from 29.1Ωm to 1644Ωm, when we compare VES 3 with ERT line 1, in VES 3 at depth 3.46m the resistivity value is 29.1 Ωm as well as in ERT line 1 at same depth the resistivity value is nearly to 29 Ωm. At lower layer of VES 3, we have the resistivity value is 1644 Ωm as well as in ERT line 1 at higher depth resistivity value is also high that correlate the VES 3 with ERT line 1.

Correlation between ERT line 4 VES 2

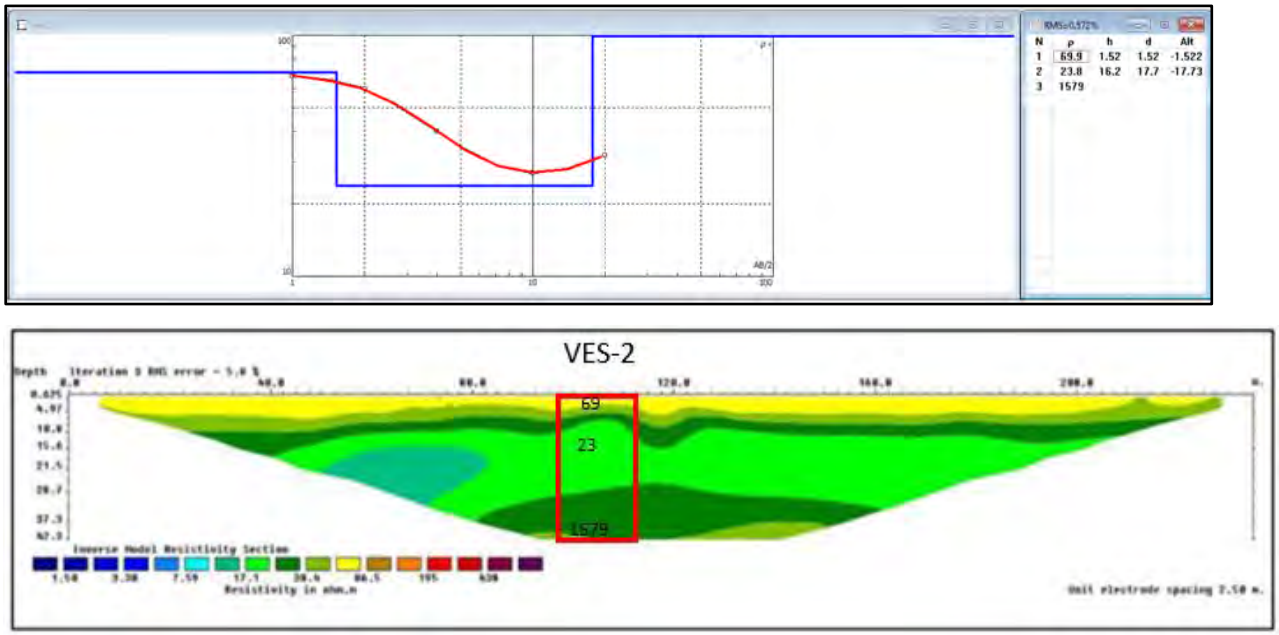

Figure-5.20 Showing correlation between ERT line 4 and VES 2.

Total depth that is investigated in VES 2 is 17.73m and resistivity is varying between 23.84Ωm to 1579Ωm and thickness of upper layer is 1.522m and resistivity is 69.95Ωm and thickness of lower layer is 16.21m and resistivity is 23.84Ωm, upper layer has higher resistivity value than lower layer figure 5.20 of ERT line 4 is confirming results of VES 2 and demonstrating correlation marked as red.

Correlation between ERT line 5 VES 1

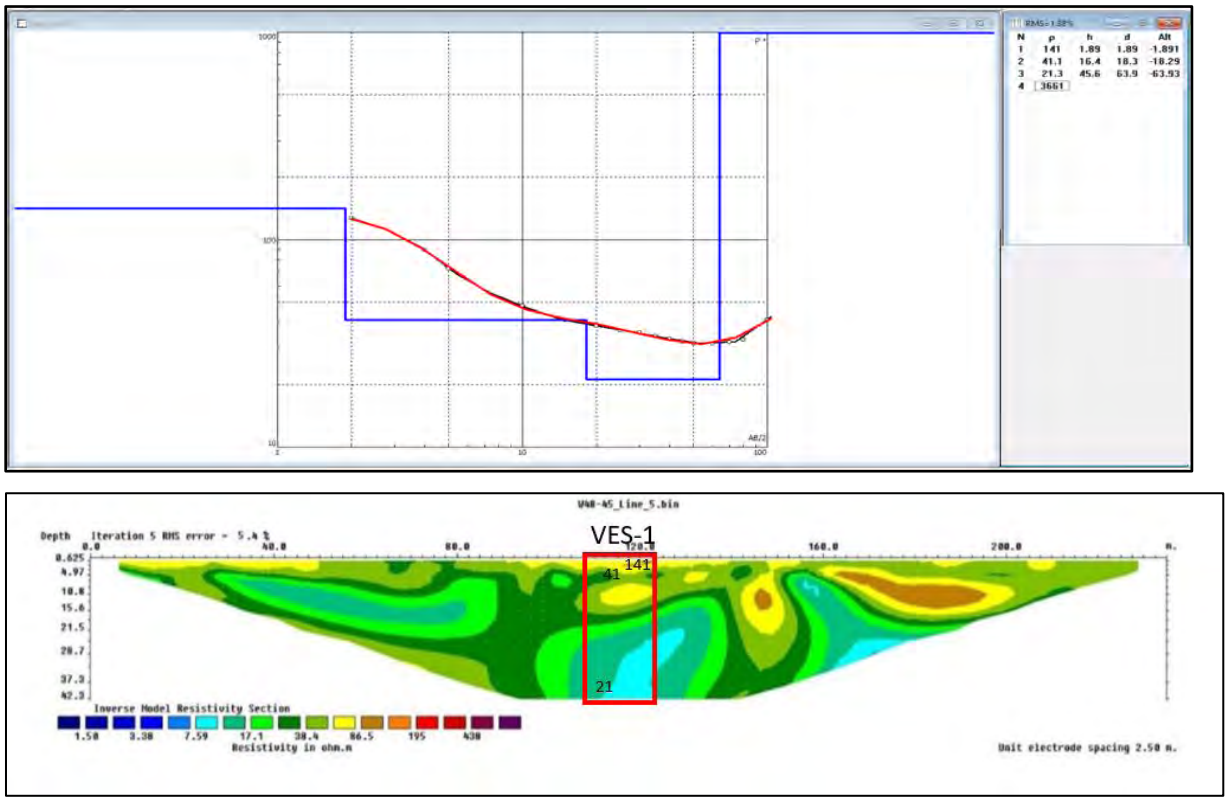

Figure-5.21 Showing correlation between ERT line 5 and VES 1.

Depth investigated altogether at VES 1 is about 63.9m meter possessing resistivity values of 21.3Ωm to 141Ωm, and also in ERT line 5 at same depth we have same resistivity value as showing figure 5.21. Similarly, in VES 1 at depth of 18.3m the resistivity value is 41 Ωm that correlate with ERT line 5 having 40 Ωm at depth of 18m. we got the low resistivity value in both cases at higher depth that confirm our result as shown in above figure 5.21.

Correlation between ERT line 6 VES 4

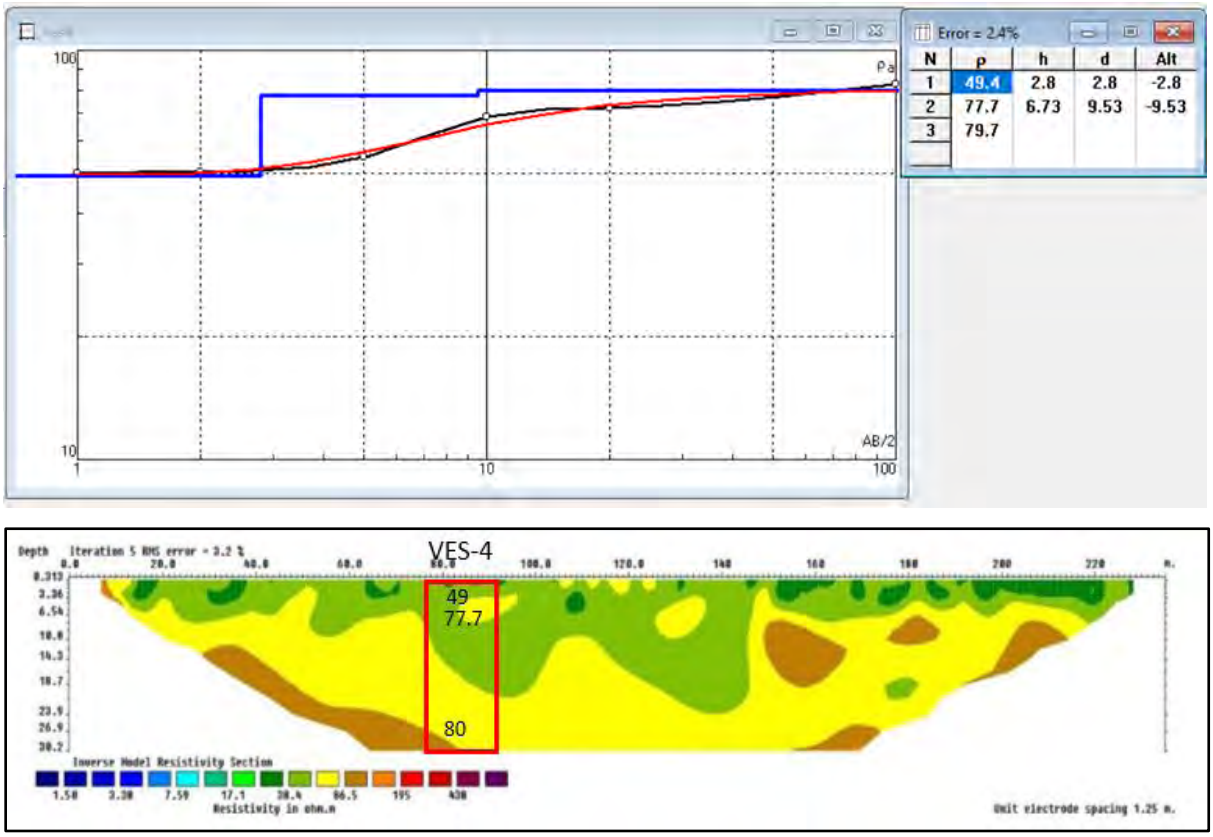

Figure-5.22 Showing correlation between ERT line 6 and VES 4.

Total depth acquired in VES 4 is 9.53m. Resistivity values in VES 4 ranging from 49.4 Ωm to 77.7 Ωm. In VES 4 we are not getting less than 30 Ωm and also in ERT line 6 we are not finding any low resistive zone that correlate with each other as showing in figure 5.22.

Type of curves and correlation according to Resistivity

- **H type curves:** are the curves in which first layer has resistivity greater then second layer and resistivity of second layer is less than third layer VES 2 and 3 is showing H type curve because VES 2 has resistivity of first layer is 69.9 **Ωm**, resistivity of second layer is 23.9 **Ωm** and of third layer is 1579 **Ωm** and in VES 3 resistivity of first layer is 29.1 **Ωm**, second layer is 7.16 **Ωm** and third layer is 1699 **Ωm**
- **A type curves:** are the curves in which resistivity of third layer is greater than resistivity of first and second layer. VES 4 is showing A type because resistivity of first layer is 49.4 **Ωm**, second layer is 77.7 **Ωm** and of third layer is 79.7 **Ωm**
- **Q type curves:** are the curves in which layer one has resistivity greater than second and third layer VES 1 is showing type Q curve in which first layer has 141 **Ωm**, layer second has resistivity of 41.10 **Ωm** and third layer has resistivity value of 21.3 **Ωm**

Chapter 6 Results and Discussion

6.1 Physiochemical parameters:

Physicochemical parameters refer to physical and chemical characteristics of a substance or system, including water. In the context of water quality, physicochemical parameters are measurements of physical and chemical properties that help to determine the quality of water and its suitability for different uses. Some of the common physicochemical parameters used to assess water quality include:

PH: property of the acid or alkaline measurement of the water. The pH scale lies from 0 to 14, and pH aproximately7 is assumed as neutral, pH less than 7 asumed as acidic, and pH more than 7 lies in basic range.

Total dissolved solids (TDS): TDS is a measure of the total amount of dissolved substances in water, including minerals, salts, and other organic and inorganic compounds.

Dissolved oxygen (DO): It is the amount of oxygen that is dissolved in water and is essential for aquatic life. DO is affected by temperature, pressure, and the level of pollutants in the water.

Biochemical oxygen demand (BOD): It is a measure of the amount of oxygen that is required by microorganisms to break down organic matter in water.

Chemical oxygen demand (COD): It is a measure of the amount of oxygen required to oxidize organic and inorganic substances in water.

Turbidity: It is a measure of the cloudiness or haziness of water caused by suspended particles.

Conductivity: It is a measure of the ability of water to conduct an electric current, which is related to the number of dissolved salts and minerals in the water.

These physicochemical parameters are often used in combination with other biological and ecological indicators to assess the overall health and quality of water.

6.2 Comparison of Parameters with WHO limits:

The collected groundwater samples from different locations were analyzed for various parameters, including electrical conductivity (EC), total dissolved solids (TDS), pH, bicarbonate (HCO3), calcium (Ca), magnesium (Mg), chloride (Cl), sulfate (SO4), hardness, sodium (Na), potassium (K), fluoride (F), and arsenic (As), nitrate (NO3), phosphate (PO4), and iron (Fe). The results showed that 39% of the samples were within WHO limits for EC, while 61% exceeded the limits with an average value of 1013µS/cm. Similarly, 32% of the samples were within WHO limits for TDS, while 68% exceeded the limits with an average value of 525.2 mg/L.

All samples were within WHO limits for ph. However, 69% of the samples exceeded WHO limits for HCO3 with an average value of 424.4 mg/L. Both Ca and Mg were 100% within WHO limits with an average value of 75.57 mg/L and 40.90 mg/L, respectively. For Cl and SO4, 87% and 86% of the samples were within WHO limits, while 13% and 14% exceeded the limits with an average value of 115.9 mg/L and 248.1 mg/L, respectively.

The hardness of 84% of the samples were within WHO limits, while 16% exceeded the limits with an average value of 352.9 mg/L. Na and K were within WHO limits for 79% and 80% of the samples, respectively, while 21% and 20% exceeded the limits with an average value of 218.8 mg/L and 8.07 mg/L, respectively. F was within WHO limits for 89% of the samples, while 11% exceeded the limits with an average value of 0.56 mg/L.

As was within WHO limits for 5% of the samples, while 95% exceeded the limits with an average value of 8.78 ppm. Finally, NO3, PO4, and Fe were 100% within WHO limits with an average value of 1.70 mg/L, 0.07 mg/L, and 0.12 mg/L, respectively.

Table-6.1 Showing physio-chemical parameters along with comparison of WHO limits

Parameters	Units	Min	Max	Avg	WHO	Percentage (%) within Limits	Percentage (%) Exceeds limit
EC	µS/cm	125	1479	1013	1000	39%	61%
TDS	mg/L	65	765	525.2	500	32%	68%
PH	----	6.15	9.62	7.89	6.5–8.5	100%	0
HCO_3	mg/L	132	678	475.27	500	37%	63%
Cl	mg/L	117	611	242.71	200	29%	71%
SO_4	mg/L	76	853	261.98	200	46%	54%
Ca	mg/L	46	422	152	100	37%	63%
Mg	mg/L	14	206	40.15	50	44%	56%
Hardness	mg/L	45	761	375.6	500	85%	15%
Na	mg/L	109	684	252.39	200	32%	68%
K	mg/L	3.32	7.56	5.12	12	100%	0
NO_3(N)	mg/L	0.87	9.16	5.66	11.3	100%	0
PO_4	mg/L	0.001	0.91	0.33	0.1	15%	85%
F	mg/L	0.80	1.937	0.51	4	100%	0
Fe	mg/L	0.001	0.53	0.18	0.3	83%	17%
As	(ppm)	7.89	98.7	34.49	10	5%	95%
Pb	(ppm)	0.001	0.06	0.03	15	100%	0

6.3 Comparison of Parameters with NSDWQ limits:

The study found that the electrical conductivity of the groundwater samples ranged from 125 - 1479 µS/cm. approximately 39% of the samples fell within the WHO limits, while the remaining 61% exceeded the limit, with an average value of 1013

µS/cm. The total dissolve solid (TDS) values ranged from 65 - 765 mg/L, and approximately 32% of the samples were within the WHO limits, while the remaining 68% exceeded the limit, with an average value of 525.2 mg/L. The pH values ranged from6.15 - 9.62, with an average value of 7.89, and all of the samples were within the WHO limits. The study also measured the concentration of other elements in the groundwater samples. The HCO3 concentration ranged from 132-678 mg/L, with an average value of 475.27 mg/L. Approximately 37% of the samples were within the WHO limits, while the remaining 63% exceeded the limit. The concentration of Ca and Mg ranged from 46 – 422 mg/L and 14 -206 mg/L, respectively, with an average value of 152 mg/L and 40.15 mg/L. The Cl and SO4 concentrations ranged from 117-611 mg/L and 76-853 mg/L, respectively, with approximately 49% and 59% of the samples within the WHO limits. The remaining 51% and 41% of the samples exceeded the limits, with an average value of 242.71 mg/L and 261.98 mg/L, respectively.

The hardness of the water ranged from 45 - 761 mg/L, with an average value of 375.6 mg/L. Approximately 85% of the samples were within the WHO limits, while the remaining 15% exceeded the limit. The concentration of Na and K ranged from 109 – 684 mg/L and 3.32 -7.56 mg/L, respectively, with an average value of 252.39 mg/L and 5.12 mg/L. Approximately 32% and 100% of the samples were within the WHO limits, while the remaining 68% and 0% exceeded the limit. The F concentration ranged from 0.80 –1.937 mg/L, with an average value of 0.51 mg/L. Approximately 100% of the samples werewithin the WHO limits. The study also measured the concentration of other elements such as NO3, PO4, and Fe, which ranged from 0.87 – 9.16 mg/L, 0.001 -0.913 mg/L, and 0.001 -0.53 mg/L, respectively, with an average value of 5.66 mg/L, 0.33 mg/L,and0.18mg/Lrespectively.

Table-6.2 Showing physiochemical parameters along with comparison of NSDWQ limits

Parameters	Units	Min	Max	Avg	NSDWQ	Percentage (%) within Limits	Percentage (%) Exceeds limit
EC	µS/cm	125	1479	1013	1000	39%	61%
TDS	mg/L	65	765	525.2	500	32%	68%
PH	----	6.15	9.62	7.89	6.5–8.5	100%	0
HCO_3	mg/L	132	678	475.27	500	37%	63%
Cl	mg/L	117	611	242.71	250	49%	51%
SO_4	mg/L	76	853	261.98	250	59%	41%
Ca	mg/L	46	422	152	100	100%	0
Mg	mg/L	14	206	40.15	50	100%	0
Hardness	mg/L	45	761	375.6	500	85%	15%
Na	mg/L	109	684	252.39	200	32%	68%
K	mg/L	3.32	7.56	5.12	12	100%	0%
NO_3(N)	mg/L	0.87	9.16	5.66	11.3	100%	0
PO_4	mg/L	0.001	0.91	0.33	0.1	15%	85%
F	mg/L	0.80	1.937	0.51	4	100%	0
Fe	mg/L	0.001	0.53	0.18	0.3	83%	17%
As	(ppm)	7.89	98.7	34.49	15	24%	76%
Pb	(ppm)	0.001	0.06	0.03	15	100%	0

6.4 Water quality Analysis:

6.4.1 Drinking water

Water quality can be identified by measuring various physical and chemical parameters of the water. Some of the important parameters to be tested for include electrical conductivity (EC), total dissolved solids (TDS), pH, sodium absorption ratio (SAR), bicarbonate (HCO3), calcium (Ca), magnesium (Mg), chloride (Cl), sulfate (SO4), boron (B), and heavy metals such as lead, cadmium, and arsenic. EC and TDS are the most commonly used parameters to assess the salinity of irrigation water. High levels of EC and TDS indicate the presence of dissolved salts in the water, which can affect the soil and crops. The pH of the water is also important as it can affect the solubility and availability of nutrients in the soil. SAR is another important parameter that indicates the ratio of sodium to calcium and magnesium in the water. High SAR values can lead to soil degradation and reduce crop yields. Bicarbonate concentration in the water can affect the soil pH and reduce the availability of certain nutrients. Calcium and magnesium are important nutrients for plant growth and their levels in irrigation water should be adequate. Chloride and sulfate concentrations can also impact soil quality and plant growth. Lastly, heavy metal contaminants in irrigation water can pose serious health risks to both humans and animals and should be regularly monitored. By testing these parameters and comparing them to established standards and guidelines, the quality of irrigation water can be identified, and appropriate actions can be taken to maintain soil and crop health.

6.4.2 Electrical Conductivity (EC):

Groundwater quality can be classified based on the electrical conductivity (EC) of the water, which is a measure of its ability to conduct an electrical current. Generally, water with low EC values is considered to be of good quality, while high EC values may indicate the presence of dissolved salts or other contaminants. This table shows the classification of water salinity based on electrical conductivity (EC) measurements. The EC is a measure of the number of dissolved salts and minerals in water. The lower the EC value, the lower the salinity of the water, while higher EC values indicate higher levels of salinity. The table lists five ranges of EC values, with corresponding classifications based

on the level of salinity. The first classification, Class-1, includes water with EC values between 0-250, which is considered to have low salinity and excellent quality.

The next classification, Class-2, includes water with EC values 251-750, which is classified as medium or good quality. Class-3 includes water with EC values between 751-2250, which is considered high but still permissible for most uses. Class-4 includes water with EC values between 2251-6000, which is classified as very high salinity. Finally, Class-5 includes water with EC values 6001-10,000, which is classified as extensively high salinity. The classification of water salinity based on EC values is important for determining the suitability of water for various uses, such as irrigation, drinking, or industrial processes. Understanding the level of salinity in water can help in making decisions about appropriate treatment or management strategies to maintain water quality and protect human and environmental health.

Salinity index range shows that the electrical conductivity values smaller then 750μS/cm are considered to be good for irrigation purpose. According to the calculations 7% Samples lie in class 2 consider to be good for irrigation purpose. 86% samples lie in permissible class having high salinity consider to be class 3 and the rest of the 7% samples lie in class 1 having low salinity means the water quality is excellent.

Table-6.3 Showing electrical conductivity with respect to salinity along with classification and respective percentage

S. No	EC	Water Salinity	Classification	Percentage (%)
1	0-250	Low (Excellent Quality)	Class-1	7%
2	251-750	Medium (Good)	Class-2	7%
3	751-2250	High (Permissible)	Class-3	86%
4	2251-6000	Very high	Class-4	NIL
5	6001-10,000	Extensively High	Class-5	NIL
6	10,001-20,000	Brines Week Concentration	Class-6	NIL
7	20,001-50,000	Brines Moderate Concentration	Class-7	NIL
8	50,001-100,000	Brines High Concentration	Class-8	NIL
9	>100,000	Brines Extensively High concentration	Class-9	NIL

6.4.3 Total Dissolved Solid:

TDS is a measure of the total amount of dissolved solids in water and includes minerals, salts, and other substances. The first range, less than 50-250 TDS, indicates that important minerals may be missing from the water, which could affect its quality. The second range of 250-1000 TDS is considered sweet water and is considered perfect or normal for most uses. However, water in the range of 1000-2000 TDS is not safe for household use. Finally, water with TDS levels greater than 2000 is considered completely unsafe for any use. It is important to monitor TDS levels to ensure that water quality is maintained at safe levels for the intended use.

The result of TDS shows that 7% of the groundwater samples lie between 50 to 250 values of TDS, 29% of the groundwater samples lie between 250 to 1000 values of TDS, 64% of the samples lie between 1000 to 2000 values of TDS and not even a single sample lie in the unsuitable class.

Table-6.4 Showing proportion of dissolved solids with no. of samples and percentage of TDS

Total Dissolved Solid		
TDS	**Samples**	**Percentage(%)**
<50 to 250	3	7%
250 to 1000	12	29%
1000 to 2000	26	64%
>2000	0	NIL

6.4.4 Irrigation water Quality:

Irrigation water quality is determined by various parameters such as SAR, Kelly's Ratio, Sodium Percentage, and Magnesium Hazard. These parameters are used to assess the potential impact of irrigation water on soil structure and crop growth. High levels of sodium can affect soil structure and reduce crop growth, while high levels of magnesium can cause soil dispersion, reducing water infiltration and root growth. The Sodium Percentage and Magnesium Hazard are classified into four categories each, while SAR and Kelly's Ratio are classified into three categories each. Analyzing these parameters is crucial for farmers and irrigation specialists to understand how water quality can affect soil health and crop growth. By taking appropriate measures to improve water quality, farmers can ensure sustainable agricultural practices. Thus, water quality testing and monitoring should be an integral part of any irrigation system to maintain healthy soil and promote sustainable crop growth.

6.4.5 Sodium Adsorption ratio (SAR):

Sodium Adsorption Ratio (SAR) is a measure of the relative amounts of sodium, calcium, and magnesium in irrigation water. It is an important parameter used to evaluate the potential impact of irrigation water on soil structure and crop growth. Sodium ions are positively charged and can attach themselves to soil particles, causing soil particles to repel each other, leading to soil dispersion. High levels of sodium can affect soil structure, making it harder for water and air to penetrate the soil, resulting in reduced crop growth. Calcium and magnesium ions, on the other hand, can help to maintain soil structure by neutralizing the negative charges on soil particles, leading to better soil

permeability and improved crop growth. SAR is calculated by dividing the concentration of sodium ions by the square root of the sum of the concentrations of calcium and magnesium ions. SAR values are classified into four categories: low (less than 10), medium (10-18), high (18-26), and very high (above 26). By analyzing SAR values, farmers and irrigation specialists can determine whether the irrigation water is suitable for use on a particular crop or whether treatment is required to improve the water quality.

The analysis of the Sodium Adsorption Ratio indicates that 97% of the water samples fall within the excellent category for water quality. Additionally, 3% of the samples are classified as good water quality. Not a single water sample falls into the doubtful or unsuitable categories.

Table-6.5 Showing sodium absorption ratio along with quality and percentage

S.NO	Sodium Adsorption Ratio (SAR)	Water Quality	Percentage (%)
1	<10	Excellent	97%
2	10 – 18	Good	3%
3	19 – 20	Doubtful	NIL
4	>20	Unsuitable	NIL

6.4.6 Sodium Percentage (Na%):

Sodium Percentage (Na%) is a measure of the relative amount of sodium compared to other positively charged ions, such as calcium, magnesium, and potassium, in irrigation water. It is an important parameter used to assess the potential impact of irrigation water on soil structure and crop growth. A high Sodium Percentage can lead to soil dispersion, which affects soil permeability and crop growth. When sodium ions in the water enter the soil, they can attach themselves to soil particles, causing the particles to repel each other and leading to soil dispersion. As a result, the soil structure becomes more unstable, reducing its ability to hold water and nutrients, which can impact plant growth. Na% is calculated by dividing the concentration of sodium ions by the sum of the concentrations of all the positively charged ions. Na% values are classified into four

categories: low (less than 20%), medium (20-40%), high (40-60%), and very high (above 60%). By analyzing Na% values, farmers and irrigation specialists can determine whether the irrigation water is suitable for useon a particular crop or whether treatment is required to improve the water quality.

The analysis of sodium percentages in the water samples revealed that none of the samples were classified as having excellent water quality. Approximately 34% of the samples were categorized as having good water quality, while 56% were considered permissible. About 10% of the samples fell into the doubtful category, but fortunately, none of the samples were found to be unsuitable.

Table-6.6 Showing sodium percentage along with water quality index

S. NO	Sodium Percentage (Na %)	Water Quality	Percentage (%)
1	<20	Excellent	NIL
2	20 – 40	Good	34%
3	40 – 60	Permissible	56%
4	60 – 80	Doubtful	10%
5	>80	Unsuitable	NIL

6.4.7 Magnesium hazard:

Magnesium Hazard (MH) is a measure of the potential negative effects of magnesium on soil structure and plant growth in irrigation water. It is an important parameter used to assess the suitability of irrigation water for crop growth. High levels of magnesium in irrigation water can cause soil dispersion, leading to reduced water infiltration and root growth. When magnesium ions enter the soil, they can attach themselves to soil particles and cause them to repel each other, resulting in soil dispersion. As a result, the soil structure becomes more unstable, which can reduce water infiltration, soil permeability, and root growth, all of which can impact plant growth. Magnesium Hazard is calculated by dividing the concentration of magnesium ions by the sum of the concentrations of calcium and magnesium ions and multiplying the result by

100. MH values are classified into four categories: low (less than 50%), medium (50-70%), high (70-90%), and very high (above 90%). By analyzing MH values, farmers and irrigation specialists can determine whether the irrigation water is suitable for use on a particular crop or whether treatment is required to improve the water quality. Magnesium Hazard is an important parameter that helps farmers and irrigation specialists assess the potential negative effects of magnesium on soil structure and plant growth in irrigation water. By maintaining a balance between magnesium and calcium ions, they can ensure sustainable crop growth and improve soil health.

The classification of water samples based on the magnesium hazard indicates that 71% of the samples were categorized as having suitable water quality, while 29% were classified as having harmful water quality.

Table-6.7 Magnesium hazard along with water quality classification and percentage

S. No	Magnesium Hazard (MH%)	Water Quality	Percentage (%)
1	<50	Suitable	71%
2	>50	Harmful	29%

6.4.8 Kelly's Ratio:

Kelly's Ratio is a measure of the balance between sodium and calcium ions in irrigation water. It is an important parameter used to assess the potential impact of irrigation water on soil structure and crop growth. High levels of sodium in irrigation water can displace calcium ions in the soil, leading to soil degradation. When sodium ions replace calcium ions in the soil, the soil structure becomes more unstable, leading to soil dispersion, which reduces soil permeability and can impact plant growth. Therefore, it is important to maintain a balance between sodium and calcium ions in the irrigation water.

Kelly's Ratio is calculated by dividing the concentration of sodium ions by the concentration of calcium ions. Kelly's Ratio values are classified into three categories:

low (less than 1), medium (1-2), and high (above 2). By analyzing Kelly's Ratio values, farmers and irrigation specialists can determine whether the irrigation water is suitable for use on a particular crop or whether treatment is required to improve the water quality. In summary, Kelly's Ratio is an important parameter that helps farmers and irrigation specialists maintain a balance between sodium and calcium ions in irrigation water to prevent soil degradation and promote sustainable crop growth. According to the Kelly's ratio, the results indicate that 54% of the samples were classified as having suitable water quality, while 44% were categorized as marginally suitable. The 2% of samples were found to be unsuitable remaining.

Table-6.8 Showing Kelly's ratio along with percentage and water quality index

S. No	Kelly's Ratio	Water Quality	Percentage (%)
1	<1	Suitable	54%
2	1 – 2	Marginal Suitable	44%
3	>2	Unsuitable	2%

6.4.9 Piper Plot:

The Piper plot is a graphical representation of the chemical composition of water samples, based on the relative concentrations of major cations and anions. It is divided into two triangles, one for cations and the other for anions, and used to identify dominant ions and classify water into different categories based on its chemical composition. It is a useful tool in hydro geochemistry and irrigation water analysis for identifying water sources and potential water quality issues. The plot was developed by R.K. Piper in 1944.

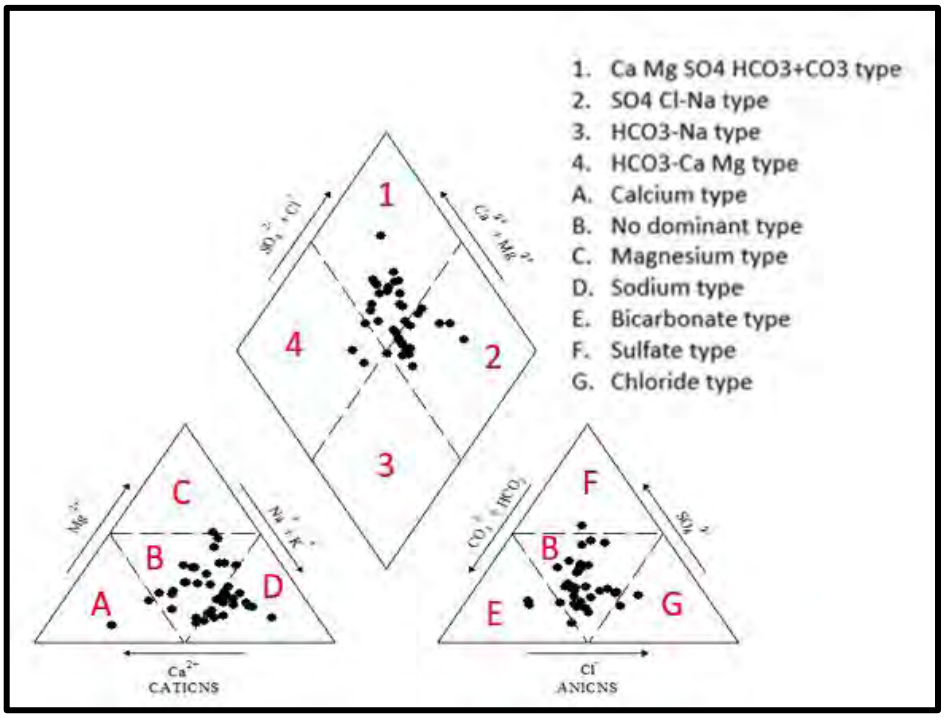

Figure-6.1 Showing piper plot having relative concentrations of major anions and cations

6.4.10 Gibbs Diagram:

The Gibbs plot is a graphical representation of the relationship between the concentration of major ions in water samples and the ratio of dissolved solids to total dissolved solids. It consists of a triangle, with the vertices representing the relative proportions of different types of water sources (rainwater, rock weathering, and evaporation). The position of the water sample on the plot indicates the dominant geochemical process controlling its composition. The Gibbs plot is often used in hydrogeology to identify the hydro geochemical processes controlling groundwater quality and to distinguish between different water sources. It was developed by W.J. Gibbs in 1970.

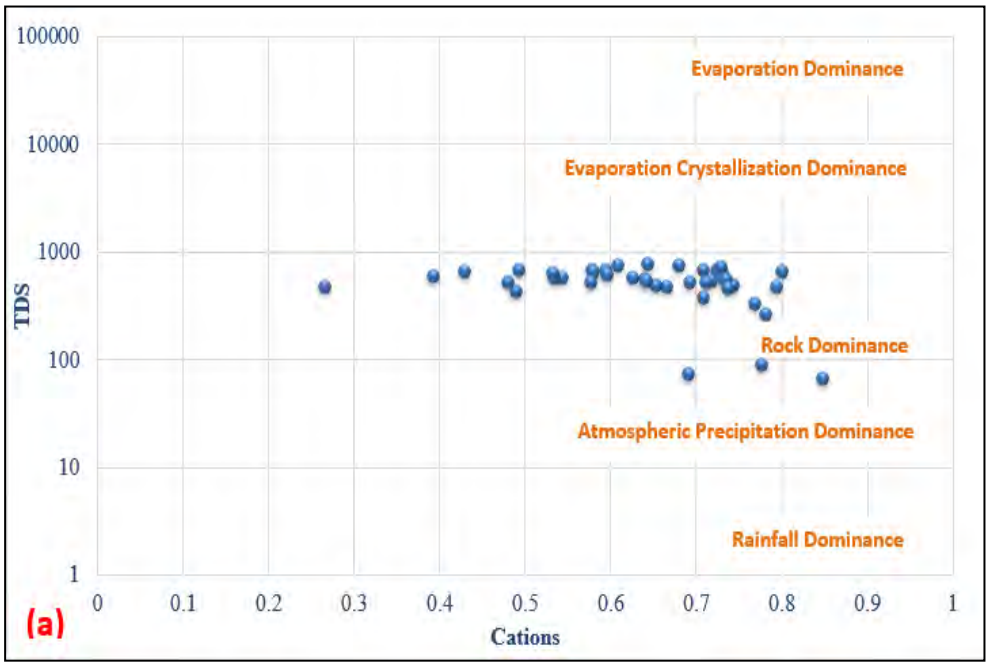

Figure-6.2 Gibbs plot showing the cat ions in water sample with respect to total dissolved solids

The Gibbs diagram categorizes water samples based on the dominant geochemical processes controlling their composition. These processes include evaporation dominance, evaporation crystallization dominance, rock dominance, atmospheric precipitation dominance, and rainfall dominance. In a study area, the cation and anion plots showed that all samples fell into the Atmospheric precipitation dominance and rock dominance zones. Most of the samples had a total dissolved solids (TDS) range between 100-1000, which is classified as a rock dominance zone, while only three samples fell into the TDS range of 10-100, indicating an atmospheric precipitation dominance zone. The majority of samples (93%) fell into the rock dominance zone, while the remaining 7% were in the atmospheric precipitation dominance zone.

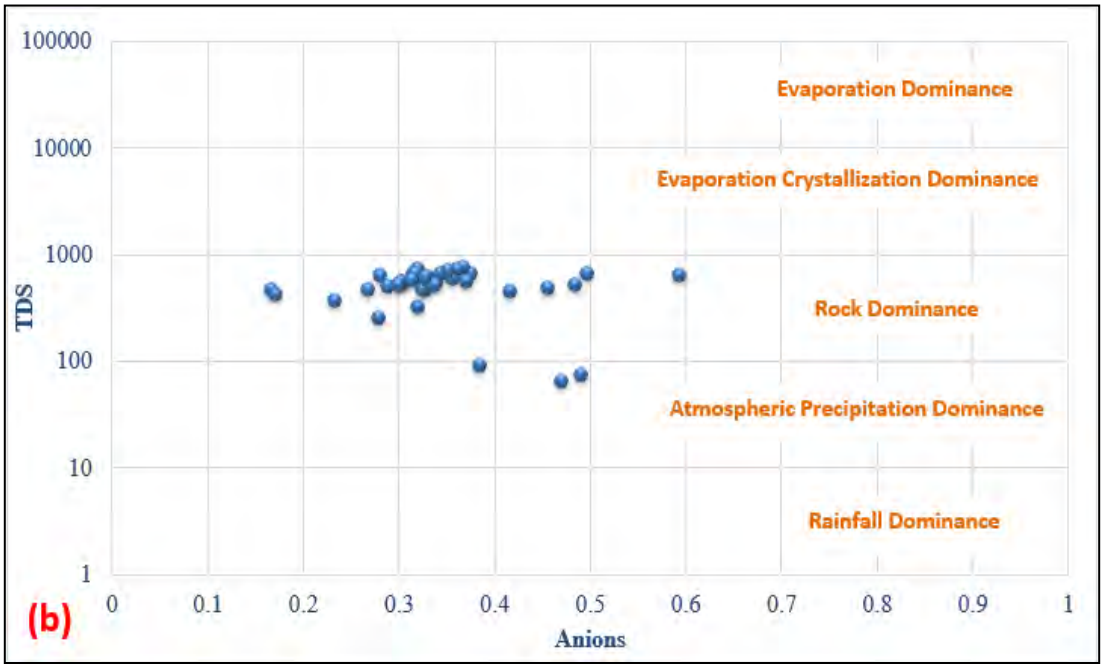

Figure-6.3 Showing Gibbs plot concentrations of ions in water with respect to dissolved solids

6.5 Water Quality Index:

Water quality index (WQI) is a measure of the overall quality of water based on various physical, chemical, and biological characteristics. The index considers several parameters such as pH, dissolved oxygen, biochemical oxygen demand, total suspended solids, temperature, conductivity, and nutrient levels, among others. The purpose of the WQI is to provide a simple and standardized way to communicate information about water quality to the public and policymakers. It helps to assess the suitability of water for various uses, such as drinking, irrigation, aquatic life, and recreation. The WQI typically uses a scale from 0 to 100, where higher values indicate better water quality. A WQI score of 100 indicates excellent water quality, while a score of 0 indicates extremely poor water quality. Several countries have developed their own versions of WQI to assess the water quality of their rivers, lakes, and other water bodies. The WQI is an important tool for monitoring and managing water resources to ensure that they are safe and sustainable for current and future generations.

The water quality index analysis are performed in this study area groundwater samples are analyzed. The water quality index analysis shows that 34% of the groundwater samples lie in the excellent class, 36% groundwater samples lie in good water quality class, 20% lie in poor class, 10% in very poor class and no sample lie in worse class.

6.6 North Side of Study area:

The results showed that 39% of the samples were within WHO limits for EC, while 61% exceeded the limits with an average value of 1013µS/cm. Similarly, 32% of the samples were within WHO limits for TDS, while 68% exceeded the limits with an average value of 525.2 mg/L. All samples were within WHO limits for pH. However, 63% of the samples exceeded WHO limits for HCO3 with an average value of 462 mg/L. Both F and Pb were 100% within WHO limits with an average value of 0.51 mg/L and 0.001 mg/L, respectively. For Ca and Mg, 37% and 44% of the samples were within WHO limits, while 63% and 56% exceeded the limits with an average value of 152 mg/L and 40.15 mg/L, respectively. The hardness of 85% of the samples was within WHO limits, while 15% exceeded the limits with an average value of 375.6 mg/L. Cl and SO4 were within WHO limits for 29% and 46% of the samples, respectively, while 71% and 54% exceeded the limits with an average value of 309 mg/L and 163.5 mg/L, respectively. F was within WHO limits for 100% of the samples. As was within WHO limits for 5% of the samples, while 95% exceeded the limits with an average value of 0.03 ppm. Finally, NO3, and K were 100% within WHO limits with an average value of 4.035 mg/L, and 5.145 mg/L, respectively.

Table-6.9 Showing water quality parameters along with standard WHO standards within and beyond limit percentages

Parameters	Units	Min	Max	Avg	WHO	Percentage (%) within Limits	Percentage (%) Exceeds limit
EC	µS/cm	125	1479	1013	1000	39%	61%
TDS	mg/L	65	765	525.2	500	32%	68%
PH	----	6.15	9.62	7.89	6.5–8.5	100%	0
HCO_3	mg/L	356	568	462	500	37%	63%
Cl	mg/L	267	351	309	200	29%	71%
SO_4	mg/L	152	175	163.5	200	46%	54%
Ca	mg/L	46	422	152	100	37%	63%
Mg	mg/L	14	206	40.15	50	44%	56%
Hardness	mg/L	45	761	375.6	500	85%	15%
Na	mg/L	109	119	114	200	32%	68%
K	mg/L	3.32	4.75	4.035	12	100%	0
NO_3(N)	mg/L	4.53	5.76	5.145	11.3	100%	0
PO_4	mg/L	0.001	0.91	0.33	0.1	15%	85%
F	mg/L	0.80	1.937	0.51	4	100%	0
Fe	mg/L	0.001	0.53	0.18	0.3	83%	17%
As	(ppm)	7.89	98.7	34.49	10	5%	95%
Pb	(ppm)	0.001	0.06	0.03	15	100%	0

6.7 South Side of Study area:

The results showed that 39% of the samples were within WHO limits for EC, while 61% exceeded the limits with an average value of 1013µS/cm. Similarly, 32% of

the samples were within WHO limits for TDS, while 68% exceeded the limits with an average value of 525.2 mg/L. All samples were within WHO limits for pH. However, 69% of the samples exceeded WHO limits for HCO3 with an average value of 424.4 mg/L. Both Ca and Mg were 100% within WHO limits with an average value of 75.57 mg/L and 40.90 mg/L, respectively. For Cl and SO4, 87% and 86% of the samples were within WHO limits, while 13% and 14% exceeded the limits with an average value of 115.9 mg/L and 248.1 mg/L, respectively. The hardness of 84% of the samples was within WHO limits, while 16% exceeded the limits with an average value of 352.9 mg/L. Na and K were within WHO limits for 79% and 80% of the samples, respectively, while 21% and 20% exceeded the limits with an average value of 218.8 mg/L and 8.07 mg/L, respectively. F was within WHO limits for 89% of the samples, while 11% exceeded the limits with an average value of 0.56 mg/L. As was within WHO limits for 49% of the samples, while 51% exceeded the limits with an average value of 8.78 ppm. Finally, NO3, PO4, and Fe were 100% within WHO limits with an average value of 1.70 mg/L, 0.07 mg/L, and 0.12 mg/L, respectively.

Table-6.10 Showing water quality parameters along with standard WHO standards within and beyond limit percentages

Parameters	**Units**	**Min**	**Max**	**Avg**	**WHO**	**Percentage (%) within Limits**	**Percentage (%) Exceeds limit**
EC	µS/cm	125	1479	1013	1000	39%	61%
TDS	mg/L	65	765	525.2	500	32%	68%
PH	----	6.15	9.62	7.89	6.5–8.5	100%	0
HCO_3	mg/L	132	678	475.27	500	37%	63%
Cl	mg/L	117	611	242.71	200	29%	71%
SO_4	mg/L	76	853	261.98	200	46%	54%
Ca	mg/L	46	422	152	100	37%	63%
Mg	mg/L	14	206	40.15	50	44%	56%
Hardness	mg/L	45	761	375.6	500	85%	15%
Na	mg/L	109	684	252.39	200	32%	68%
K	mg/L	3.32	7.56	5.12	12	100%	0
NO_3(N)	mg/L	0.87	9.16	5.66	11.3	100%	0
PO_4	mg/L	0.001	0.91	0.33	0.1	15%	85%
F	mg/L	0.80	1.937	0.51	4	100%	0
Fe	mg/L	0.001	0.53	0.18	0.3	83%	17%
As	(ppm)	7.89	98.7	34.49	10	5%	95%
Pb	(ppm)	0.001	0.06	0.03	15	100%	0

6.8 East Side of Study area:

The results showed that 39% of the samples were within WHO limits for EC, while 61% exceeded the limits with an average value of 1013µS/cm. Similarly, 32% of the samples were within WHO limits for TDS, while 68% exceeded the limits with an average value of 525.2 mg/L. All samples were within WHO limits for pH. However, 69% of the samples exceeded WHO limits for HCO3 with an average value of 424.4 mg/L. Both Ca and Mg were 100% within WHO limits with an average value of 75.57 mg/L and 40.90 mg/L, respectively. For Cl and SO4, 87% and 86% of the samples were within WHO limits, while 13% and 14% exceeded the limits with an average value of 115.9 mg/L and 248.1 mg/L, respectively. The hardness of 84% of the samples was within WHO limits, while 16% exceeded the limits with an average value of 352.9 mg/L. Na and K were within WHO limits for 79% and 80% of the samples, respectively, while 21% and 20% exceeded the limits with an average value of 218.8 mg/L and 8.07 mg/L, respectively. F was within WHO limits for 89% of the samples, while 11% exceeded the limits with an average value of 0.56 mg/L. As was within WHO limits for 49% of the samples, while 51% exceeded the limits with an average value of 8.78 ppm. Finally, NO3, PO4, and Fe were 100% within WHO limits with an average value of 1.70 mg/L, 0.07 mg/L, and 0.12 mg/L, respectively.

Table-6.11 Showing water quality parameters along with standard WHO standards at East Side of Study area

Parameters	Units	Min	Max	Avg	WHO	Percentage (%) within Limits	Percentage (%) Exceeds limit
EC	µS/cm	125	1479	1013	1000	39%	61%
TDS	mg/L	65	765	525.2	500	32%	68%
PH	----	6.15	9.62	7.89	6.5–8.5	100%	0
HCO_3	mg/L	132	678	475.27	500	37%	63%
Cl	mg/L	117	611	242.71	200	29%	71%
SO_4	mg/L	76	853	261.98	200	100%	0

Ca	mg/L	46	422	152	100	37%	63%
Mg	mg/L	14	206	40.15	50	100%	0
Hardness	mg/L	45	761	375.6	500	100%	0
Na	mg/L	109	684	252.39	200	100%	0
K	mg/L	3.32	7.56	5.12	12	100%	0
NO_3(N)	mg/L	0.87	9.16	5.66	11.3	100%	0
PO_4	mg/L	0.001	0.91	0.33	0.1	15%	85%
F	mg/L	0.80	1.937	0.51	4	100%	0
Fe	mg/L	0.001	0.53	0.18	0.3	100%	0
As	(ppm)	7.89	98.7	34.49	10	5%	95%
Pb	(ppm)	0.001	0.06	0.03	15	100%	0

6.9 West Side of Study area:

The results showed that 39% of the samples were within WHO limits for EC, while 61% exceeded the limits with an average value of 1013µS/cm. Similarly, 32% of the samples were within WHO limits for TDS, while 68% exceeded the limits with an average value of 525.2 mg/L. All samples were within WHO limits for pH. However, 69% of the samples exceeded WHO limits for HCO3 with an average value of 424.4 mg/L. Both Ca and Mg were 100% within WHO limits with an average value of 75.57 mg/L and 40.90 mg/L, respectively. For Cl and SO4, 87% and 86% of the samples were within WHO limits, while 13% and 14% exceeded the limits with an average value of 115.9 mg/L and 248.1 mg/L, respectively. The hardness of 84% of the samples was within WHO limits, while 16% exceeded the limits with an average value of 352.9 mg/L. Na and K were within WHO limits for 79% and 80% of the samples, respectively, while 21% and 20% exceeded the limits with an average value of 218.8 mg/L and 8.07 mg/L, respectively. F was within WHO limits for 89% of the samples, while 11% exceeded the limits with an average value of 0.56 mg/L. As was within WHO limits for 49% of the

samples, while 51% exceeded the limits with an average value of 8.78 ppm. Finally, NO3, PO4, and Fe were 100% within WHO limits with an average value of 1.70 mg/L, 0.07 mg/L, and 0.12 mg/L, respectively.

Table-6.12 Showing water quality parameters along with standard WHO standards at West Side of Study area

Parameters	**Units**	**Min**	**Max**	**Avg**	**WHO**	**Percentage (%) within Limits**	**Percentage (%) Exceeds limit**
EC	µS/cm	125	1479	1013	1000	89%	11%
TDS	mg/L	65	765	525.2	500	89%	11%
PH	----	6.15	9.62	7.89	6.5–8.5	11%	89%
HCO_3	mg/L	132	678	475.27	500	89%	11%
Cl	mg/L	117	611	242.71	200	100%	0
SO_4	mg/L	76	853	261.98	200	89%	11%
Ca	mg/L	46	422	152	100	89%	11%
Mg	mg/L	14	206	40.15	50	44%	56%
Hardness	mg/L	45	761	375.6	500	100%	0
Na	mg/L	109	684	252.39	200	67%	33%
K	mg/L	3.32	7.56	5.12	12	100%	0
NO_3(N)	mg/L	0.87	9.16	5.66	11.3	100%	0
PO_4	mg/L	0.001	0.91	0.33	0.1	11%	89%
F	mg/L	0.80	1.937	0.51	4	100%	0
Fe	mg/L	0.001	0.53	0.18	0.3	83%	17%
As	(ppm)	7.89	98.7	34.49	10	5%	95%
Pb	(ppm)	0.001	0.06	0.03	15	100%	0

6.10 Southeast side of Study area:

The results showed that 39% of the samples were within WHO limits for EC, while 61% exceeded the limits with an average value of 1013µS/cm. Similarly, 32% of the samples were within WHO limits for TDS, while 68% exceeded the limits with an average value of 525.2 mg/L. All samples were within WHO limits for pH. However, 69% of the samples exceeded WHO limits for HCO3 with an average value of 424.4 mg/L. Both Ca and Mg were 100% within WHO limits with an average value of 75.57 mg/L and 40.90 mg/L, respectively. For Cl and SO4, 87% and 86% of the samples were within WHO limits, while 13% and 14% exceeded the limits with an average value of 115.9 mg/L and 248.1 mg/L, respectively. The hardness of 84% of the samples was within WHO limits, while 16% exceeded the limits with an average value of 352.9 mg/L. Na and K were within WHO limits for 79% and 80% of the samples, respectively, while 21% and 20% exceeded the limits with an average value of 218.8 mg/L and 8.07 mg/L, respectively. F was within WHO limits for 89% of the samples, while 11% exceeded the limits with an average value of 0.56 mg/L. As was within WHO limits for 49% of the samples, while 51% exceeded the limits with an average value of 8.78 ppm. Finally, NO3, PO4, and Fe were 100% within WHO limits with an average value of 1.70 mg/L, 0.07 mg/L, and 0.12 mg/L, respectively.

Table-6.13 Showing water quality parameters along with standard WHO standards at Southeast side of Study area

Parameters	Units	Min	Max	Avg	WHO	Percentage (%) within Limits	Percentage (%) Exceeds limit
EC	µS/cm	125	1479	1013	1000	17%	83%
TDS	mg/L	65	765	525.2	500	11%	89%
PH	----	6.15	9.62	7.89	6.5–8.5	100%	0
HCO_3	mg/L	132	678	475.27	500	17%	83%
Cl	mg/L	117	611	242.71	200	0	100%
SO_4	mg/L	76	853	261.98	200	33%	67%
Ca	mg/L	46	422	152	100	17%	83%
Mg	mg/L	14	206	40.15	50	22%	78%
Hardness	mg/L	45	761	375.6	500	83%	17%
Na	mg/L	109	684	252.39	200	17%	83%
K	mg/L	3.32	7.56	5.12	12	100%	0
NO_3(N)	mg/L	0.87	9.16	5.66	11.3	100%	0
PO_4	mg/L	0.001	0.91	0.33	0.1	17%	83%
F	mg/L	0.80	1.937	0.51	4	100%	0
Fe	mg/L	0.001	0.53	0.18	0.3	83%	17%
As	(ppm)	7.89	98.7	34.49	10	17%	83%
Pb	(ppm)	0.001	0.06	0.03	15	100%	0

6.11 Arsenic Distribution map:

Arsenic can be highly toxic to humans and animals, depending on the dose and form in which it is consumed. Inorganic arsenic, which is often found in contaminated water and food, is the most toxic form of the element. Chronic exposure to arsenic can lead to a variety of health problems, including skin lesions, cancers of the bladder, lung,

and skin, and cardiovascular disease. Despite its toxicity, arsenic has some useful applications. It is used in small amounts in some medications to treat certain conditions, and it is also used in the production of certain alloys and pigments.

A spatial distribution map was created to identify the distribution of arsenic. The World Health Organization (WHO) has set a limit of 10mg/l for arsenic, and values ranging from 0 to 10mg/l are considered to have low arsenic concentration, represented by dark green color. Values greater than 10mg/l are considered to have high arsenic concentration and are represented by light green to white colors. The map shows that only 5% of the samples collected had arsenic concentrations within the WHO limit, while 95% of the samples exceeded the limit.

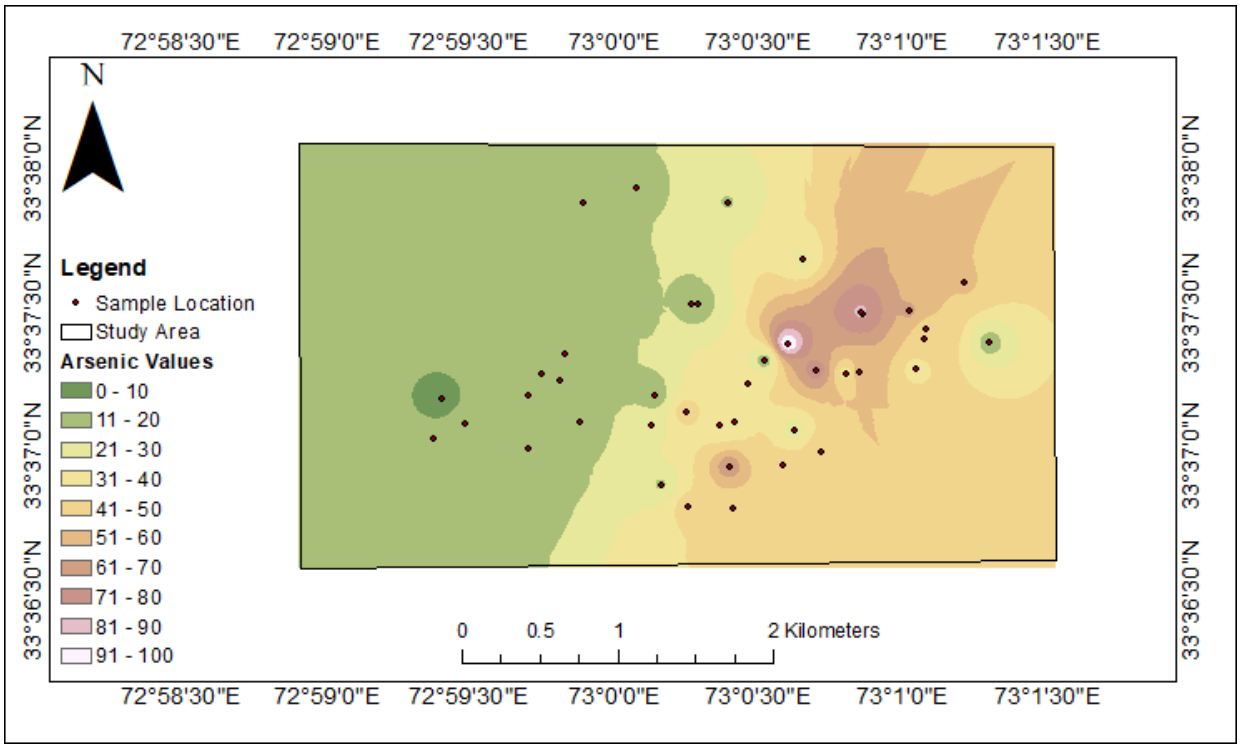

Figure-6.4 Showing spatial arsenic distribution low to high concentration is shown with color variations

6.12 Hazard Quotient analysis:

Hazard quotient (HQ) is a measure used in toxicology to estimate the risk of adverse health effects resulting from exposure to a chemical or toxic substance. HQ is calculated by dividing the level of exposure to a chemical by the reference dose (RfD) of that chemical. The RfD is an estimate of the daily dose of a chemical that is unlikely to cause any adverse health effects over a lifetime of exposure. If the HQ value is greater than 1, it suggests that there may be a risk of adverse health effects from exposure to that chemical. In contrast, an HQ value of less than 1 indicates that the exposure is unlikely to result in any significant health effects. The limits for HQ vary depending on the chemical or substance being studied, as well as the population being exposed. Generally, an HQ of less than 1 is considered to be safe, while an HQ of greater than 1 suggests that further evaluation and risk management strategies may be needed to reduce the risk of adverse health effects. However, the interpretation of HQ values should be done carefully, taking into account other factors such as the nature, duration, and frequency of exposure, as well as individual susceptibilities and other potential sources of exposure.

According to the map, nearly 95% of the groundwater samples analyzed have Hazard Quotient (HQ) values greater than 1, indicating a potential risk of adverse health effects from exposure to the analyzed substances. Only 5% of the samples have HQ values lower than 1, suggesting that the exposure to the analyzed substances in these samples is unlikely to result in significant health effects.

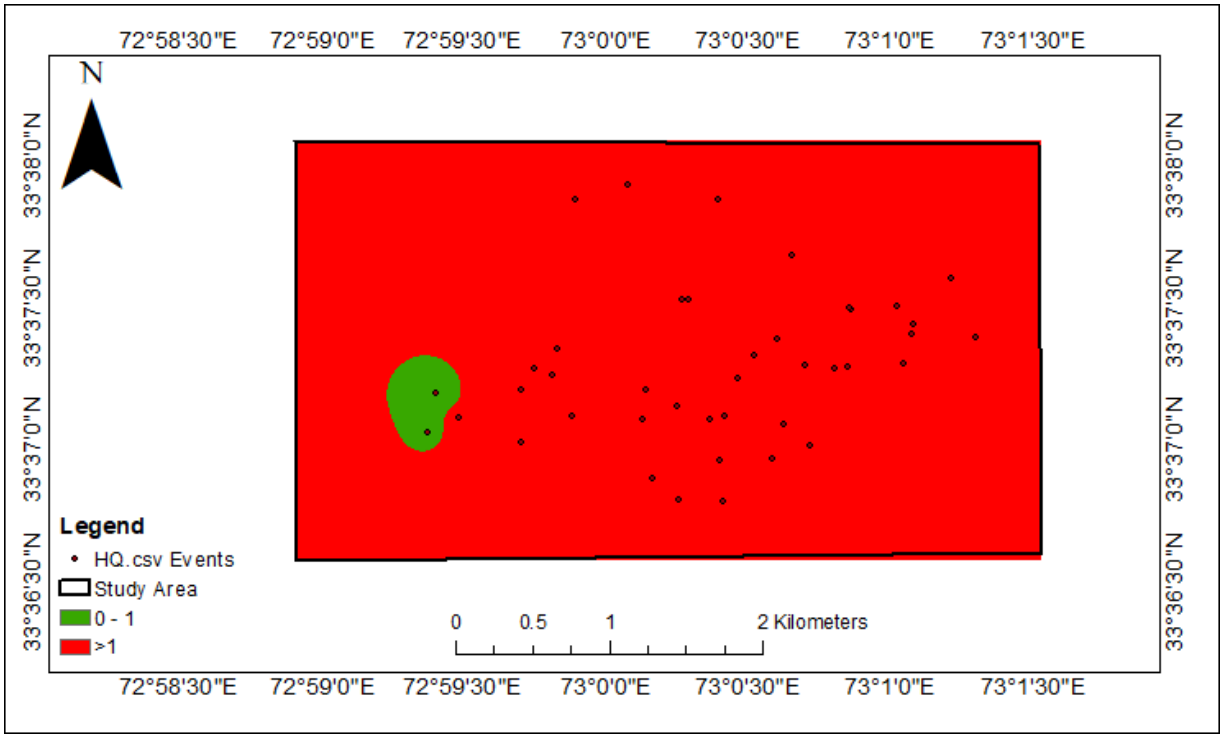

Figure-6.5 Hazard quotient map showing percentage values for health effects

Correlation between ERT and water quality

Table 6.14 showing correlation between ERT and water sample

Sample No	Electrical Conductivity µS/cm	Total Dissolved Solid mg/L	Electrical Resistivity Imaging	Value
1	172	89	Line 6	High
2	139	73	Line 6	High
3	1228	638	Line 3	Low
4	1274	662	Line 3	Low

ERT line 3

ERT line 3 is acquired at main dump site, sample no 3 and 4 is nearest to ERT line 3, (Wadhah M. Shakir (2021)) where the resistivity comes to be low, but the value of electrical conductivity (EC) and total dissolved solvent (TDS) is higher. EC and TDS are 1228 µS/cm and 632mg/L for sample 3 and 1274µS/cm and 662mg/L for sample 4 so these parameters is correlating in our study area.

In ERT line 3 lowest resistivity value obtained is 17Ωm and the overall resistivity is not more

than 38Ωm TDS and EC value near this profile is higher so the water samples and ERT is correlating in our study

ERT line 6

ERT line 6 ERT profile 6 is acquired in north of waste site in northeast-southwest. Inversion result is shown in figure 5.16.This profile is acquired at upstream relative to the waste site. Resistivity values of equal to or less than 30 Ωm are not present in the section sample 1 and 2 is nearest to line 6 where resistivity value obtained is highest but the value of electrical conductivity (EC) and total dissolved solvent (TDS) is lower. EC and TDS are 172 µS/cm and 89mg/L for sample 1 and 139 µS/cm and 73mg/L for sample 2. Resistivity value obtained is maximum 190 Ωm.

6.13. Conclusions

- The main contamination lies in ERT profile 1, 2, 3, and 4. ERT profile 5 and 6 wereacquired away from contamination area,
- Study found out that as 5 and 6 profile is away from open dump site it contains less pollution
- It concluded that upstream area does not have contamination in ground water but downstream side has more contamination
- Water quality and ERT have confirmed results that upstream side having profile 5 and 6 are safe as compared to downstream side
- Depth of leachate was analyzed that showed that it penetrated about 35 to 40 meters in groundwater
- ERT is useful for identification of leachate. ERT also helpful for determining depth and thickness of leachate in subsurface.
- VES is useful for identification of leachate. VES data can show depth of leachate and thickness from apparent resistivity values.

- In our study area, depth of penetration of VES is observed to be equal to half of the given reading spread.

  Depth of penetration = AB/2
- VES is not good for making layer model of contaminated subsurface because abrupt changes in resistivity values due to leachate lead to poor curve fitting.
- Nearly 95% of the groundwater samples analyzed have Hazard Quotient (HQ) values greater than 1, indicating a potential risk of adverse health effects from exposure to the analyzed substances
- Water quality analysis have shown that arsenic and chlorine concentrations in downstream side are more than standard safe values recommended by WHO so water should be treated for human consumption otherwise it can cause serious health hazards

References:

Aitken, M. J. (1974). Physics and archaeology.

Barker, R. J. F. b. (1992). A simple algorithm for electrical imaging of the subsurface. *10*(2).

Binley, A., Hubbard, S. S., Huisman, J. A., Revil, A., Robinson, D. A., Singha, K., & Slater, L. D. J. W. r. r. (2015). The emergence of hydro geophysics for improved understanding of subsurface processes over multiple scales. *51*(6), 3837-3866.

Dahlin, T., & Zhou, B. J. G. p. (2004). A numerical comparison of 2D resistivity imaging with 10 electrode arrays. *52*(5), 379-398.

Daily, W., & Owen, E. J. G. (1991). Cross-borehole resistivity tomography. *56*(8), 1228-1235.

Daniels, D., Gunton, D., & Scott, H. (1988). *Introduction to subsurface radar*. Paper presented at the IEE Proceedings F (Communications, Radar and Signal Processing).

Griffiths, D., & Barker, R. J. J. o. a. G. (1993). Two-dimensional resistivity imaging and modelling in areas of complex geology. *29*(3-4), 211-226.

Habberjam, G. J. G. p. (1975). Apparent resistivity, anisotropy and strike measurements. *23*(2), 211-247.

Heenan, J., Slater, L. D., Ntarlagiannis, D., Atekwana, E. A., Fathepure, B. Z., Dalvi, S., et al. (2015). Electrical resistivity imaging for long-term autonomous monitoring of hydrocarbon degradation: Lessons from the Deepwater Horizon oil spill. *80*(1), B1-B11.

Kearey, P., Brooks, M., & Hill, I. (2002). *An introduction to geophysical exploration* (Vol. 4): John Wiley & Sons.

Loke, M., & Barker, R. J. G. (1995). Least-squares deconvolution of apparent resistivity pseudosections. *60*(6), 1682-1690.

McNeil, J. J. G. L., Ontario, Canada, 22p. (1980). Electrical Conductivity of Soils and Rocks, Technical note TN-5.

Mehdi, M., and Samaei, M.R., 2017. Investigation of groundwater due to heavy metal contamination using vertical electrical sounding (VES) method. Journal of Applied Geophysics, 143, pp.72-82.

Olayinka, A., & Barker, R. J. G. (1990). Borehole Siting in Crystalline Basement Areas of Nigeria with a Microprocessor- Controlled Resistivity Traversing System. *28*(2), 178-183.

Parasnis, D. S. (2012). *Principles of applied geophysics*: Springer Science & Business Media.

Pratt, T. L., Çoruh, C., Costain, J. K., & Glover III, L. J. J. o. G. R. S. E. (1988). A geophysical study of the Earth's crust in central Virginia: Implications for Appalachian crustal structure. *93*(B6), 6649-6667.

Rogers, R. B., & Kean, W. F. J. G. (1980). Monitoring ground- water contamination at a fly ash disposal site using surface electrical resistivity methods. *18*(5), 472-478.

Safeeq, M., & Fares, A. J. E. i. i. g. r. (2016). Groundwater and surface water interactions in relation to natural and anthropogenic environmental changes. 289-326.

Shanmugam, G. (2025). Symposium Talk:" Recent advances in interpreting deep-marine deposits.

Sumner, J. S. (2012). *Principles of induced polarization for geophysical exploration*: Elsevier.

Tagg, G. J. E. 一. Earth Resistances (1964) George Newnes Limited (9) 高橋･美多･川瀬:「並列接地の集合係数について」, 電気学会電力応用研資. 78-75.

Telford, W. M., Telford, W., Geldart, L., & Sheriff, R. E. (1990). *Applied geophysics*: Cambridge university press.

Thanassoulas, C., Tsokas, G., & Kolios, N. J. G. (1987). Geophysical investigations in the geothermal field in the Delta of the Nestos river (northern Greece). *16*(1), 17-26.

Thiele, S. T., Lorenz, S., Kirsch, M., Acosta, I. C. C., Tusa, L., Herrmann, E., et al. (2021). Multi-scale, multi-sensor data integration for automated 3-D geological mapping. *136*, 104252.

Van, G. P., Park, S. K., & Hamilton, P. (1992). *Use of resistivity monitoring systems to detect leaks from storage ponds.* Paper presented at the 5th EEGS Symposium on the Application of Geophysics to Engineering and Environmental Problems.

Ward, S. H. (1988). *The resistivity and induced polarization methods.* Paper presented at the 1st EEGS Symposium on the Application of Geophysics to Engineering and Environmental Problems.

Ward, S. H., & Hohmann, G. W. (1988). Electromagnetic theory for geophysical applications. In *Electromagnetic Methods in Applied Geophysics: Voume 1, Theory* (pp. 130-311): Society of Exploration Geophysicists.

Zohdy, A. A., Eaton, G. P., & Mabey, D. R. (1974). Application of surface geophysics to ground-water investigations.

Khan, S. J., Javed, A., Ali, S. S., & Akram, M. R. (2015). Groundwater recharge and hydrogeochemistry of the Margalla Hills Range, Islamabad, Pakistan. Environmental Earth Sciences, 74(1), 199-211.

qbal M.sheikh, m. k. (2007). environmental geology of islamabad rawalpindi northern pakistan. In P. D. Wardlaw, *regional studies of potwar plateau area northern pakistan* (p. chapter G). virginia: U.S geological survey.

S. MUNIR, *. M. (2011). ASSESSMENT OF GROUNDWATER QUALITY USING PHYSIOCHEMICAL AND. *The Nucleus*, 149-158.

Wardlaw, P. D. (2007). *Regional Studies of the potwar plateau area north pakistan.* USGS.

Yang, C., Zhang, J., Chen, X., Chen, W. and Wu, J., 2011. Detection of subsurface heterogeneity in a contaminated site using electrical resistivity tomography and vertical electrical sounding methods. Journal of Applied Geophysics, 75(4), pp.733-743.

zahir, a. (2020). Hydrogeophysical investigation for groundwater potential through Electrical Resistivity Survey in Islamabad, Pakistan. *JOURNAL OF GEOGRAPHY AND SOCIAL SCIENCES*, 17 .

Zeeshan, M. T. (2020). Hydrogeophysical investigation for groundwater potential. *journal of geology and social sciences*, 147-163.